

VIBRATION AND BUCKLING ANALYSIS OF CRACKED COMPOSITE BEAM

**A THESIS SUBMITTED IN PARTIAL FULFILLMENT OF
THE REQUIREMENTS FOR THE DEGREE OF**

Master of Technology

In

Structural Engineering

By

Pragyan Saraswati Bisi

ROLL NO. 209CE2037



**DEPARTMENT OF CIVIL ENGINEERING
NATIONAL INSTITUTE OF TECHNOLOGY
ROURKELA-769008**

MAY 2011

“VIBRATION AND BUCKLING ANALYSIS OF CRACKED COMPOSITE BEAM”

A THESIS SUBMITTED IN PARTIAL FULFILLMENT OF
THE REQUIREMENTS FOR THE DEGREE OF

Master of Technology

In

Structural Engineering

By

Pragyan Saraswati Bisi

Roll No. 209CE2037

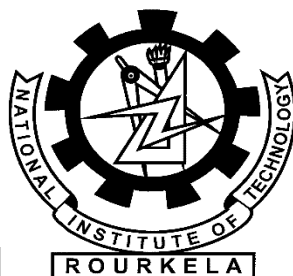
Under the guidance of

Prof. U. K. Mishra & Prof. S. K. Sahu



**DEPARTMENT OF CIVIL ENGINEERING
NATIONAL INSTITUTE OF TECHNOLOGY
ROURKELA-769008**

MAY 2011



NATIONAL INSTITUTE OF TECHNOLOGY

ROURKELA

CERTIFICATE

*This is to certify that the thesis entitled, “**VIBRATION AND BUCKLING ANALYSIS OF CRACKED COMPOSITE BEAM**” submitted by **Ms. Pragyan Saraswati Bisi** in partial fulfillment of the requirements for the award of Master of Technology Degree in Civil Engineering with specialization in “Structural Engineering” at National Institute of Technology, Rourkela is an authentic work carried out by her under my supervision and guidance. To the best of my knowledge, the matter embodied in this thesis has not been submitted to any other university/ institute for award of any Degree or Diploma.*

Prof. Shishir Kumar Sahu

Dept. of Civil Engineering

National Institute of Technology,

Rourkela - 769008

Prof. Uttam Kumar Mishra

Dept. of Civil Engineering

National Institute of Technology,

Rourkela - 769008

ACKNOWLEDGEMENT

It is with a feeling of great pleasure that I would like to express my most sincere heartfelt gratitude to my guides, **Prof. Uttam Kumar Mishra** and **Prof. Shishir Kumar Sahu**, professors, Dept. of Civil Engineering, NIT, Rourkela for their encouragement, advice, mentoring and research support throughout my studies. Their technical and editorial advice was essential for the completion of this dissertation. Their ability to teach, depth of knowledge and ability to achieve perfection will always be my inspiration.

I express my sincere thanks to **Prof. S. K. Sharangi**, Director of NIT, Rourkela & **Prof. M. Panda**, Professor and HOD, Dept. of Civil Engineering NIT, Rourkela for providing me the necessary facilities in the department.

I would also take this opportunity to express my gratitude and sincere thanks to **Prof. A. V. Asha**, my faculty and adviser and all faculty members of structural engineering, **Prof. M. R. Barik**, **Prof. K. C. Biswal** for their invaluable advice, encouragement, inspiration and blessings during the project.

I would like to thank my friends **Nemi, Anil (from IIK)** for taking time with me to discuss my research problem. Your long-term support and encouragement are truly appreciated. I would also express my sincere thanks to laboratory Members of Department of Civil Engineering, NIT, Rourkela.

Last but not the least I would like to thank my parents, who taught me the value of hard work by their own example. I would like to share this bite of happiness with my father **Dr. Amulya Kumar Bisi (M.D. Medicine)** and my mother **Dr. Madhuri Purohit (M.D. SPM.)**. They rendered me enormous support during the whole tenure of my stay at NIT, Rourkela.

Pragyan Saraswati Bisi

Roll No. - 209CE2037

CONTENTS

	Pages
1 INTRODUCTION	1-4
1.1 Introduction	1
1.2 Present Investigation	4
2 LITERATURE REVIEWS	5-12
2.1 Introduction	5
2.2 Review on vibration of cracked composite beam	5
2.3 Review on buckling analysis of composite cracked beam	10
3 THEORY AND FORMULATIONS	13-29
3.1 Introduction	13
3.2 The Methodology	13
3.3 Governing Equation	14
3.4 Mathematical Model	16
3.4.1 Buckling analysis studies	16
3.4.2 Derivation of Element Matrices	17
3.4.2.1 Stress-Strain matrix	18
3.4.2.2 Element stiffness matrix	18
3.4.2.3 Generalized element mass matrix	20
3.4.2.4 Geometrical stiffness matrix	21
3.4.2.5 Stiffness matrix for cracked composite beam element	22
3.5 Computational procedure for a cracked composite beam	28

3.5.1	Flow Chart of the program	29
4	RESULTS AND DISCUSSIONS	30-58
4.1	Introduction	30
4.2	Convergence Study	31
4.3	Comparison with Previous Studies	33
4.3.1	Vibration analysis studies	33
4.3.2	Buckling analysis studies	38
4.4	Numerical Results	39
4.4.1(A)	Vibration analysis of results of composite beam with single crack	40
4.4.1(B)	Vibration analysis of results of composite beam with multiple cracks	54
4.4.2	Buckling analysis of results of composite beam with single crack	56
5	CONCLUSION	60-61
5.1	Conclusion	60
5.2	Scope of future works	61
6	REFERENCE	62-64
7	Appendix –A	65-66

ABSTRACT

Cracks in structural members lead to local changes in their stiffness and consequently their static and dynamic behaviour is altered. The influence of cracks on dynamic characteristics like natural frequencies, modes of vibration of structures has been the subject of many investigations. However studies related to behavior of composite cracked structures subject to in-plane loads are scarce in literature. Present work deals with the vibration and buckling analysis of a cantilever beam made from graphite fiber reinforced polyimide with a transverse one-edge non-propagating open crack using the finite element method. The undamaged parts of the beam are modeled by beam finite elements with three nodes and three degrees of freedom at the node. An ‘overall additional flexibility matrix’ is added to the flexibility matrix of the corresponding non-cracked composite beam element to obtain the total flexibility matrix, and therefore the stiffness matrix in line with previous studies. The vibration of cracked composite beam is computed using the present formulation and is compared with the previous results. The effects of various parameters like crack location, crack depth, volume fraction of fibers and fibers orientations upon the changes of the natural frequencies of the beam are studied. It is found that, presence of crack in a beam decreases the natural frequency which is more pronounced when the crack is near the fixed support and the crack depth is more. The natural frequency of the cracked beam is found to be maximum at about 45% of volume fraction of fibres and the frequency for any depth of crack increases with the increase of angle of fibres. The static buckling load of a cracked composite beam is found to be decreasing with the presence of a crack and the decrease is more severe with increase in crack depth for any location of the crack. Furthermore, the buckling load of the beam decreased with increase in angle of the fibres and is maximum at 0 degree orientation.

LIST OF FIGURES

Figure No.		Pages
Figure.3.1	Schematic diagram cantilever composite beam with a crack	16
Figure.3.2	Nodal displacements in the element coordinate system	18
Figure.3.3	A typical cracked composite beam element subjected to shearing	23
Figure.3.4	Geometry of a finite composite beam element with an open crack	27
Figure.3.5	Program Flow Chart	29
Figure.4.1	Geometry of cantilever cracked composite beam with 12 elements	31
<u>Convergence study :</u>		
Figure.4.2	The convergence of non-dimensional free vibration frequencies of cracked composite beam for angle of fibers " $\alpha = 0$ " (degrees)	32
<u>Comparison with previous studies :</u>		
Figure.4.3	First three non-dimensional frequencies of the non-cracked composite beam as a function of the angle of fibers α . Values of V: 0.1	35
Figure.4.4	First three non-dimensional frequencies of the non-cracked composite beam as a function of the angle of fibers α . Values of V: 0.30	35
Figure.4.5	Changes in the first non-dimensional natural frequencies of the cracked composite beam as a function of the angle of fibers α for several values of the crack depth $a/H = 0.0, 0.2, 0.4$ and 0.6 (value fraction of fibers $V = 10\%$, crack location $x/L = 0.1$)	37
Figure.4.6	Changes in the second non-dimensional natural frequencies of the cracked composite beam as a function of the angle of fibers α for several values of the crack depth $a/H = 0.0, 0.2, 0.4$ and 0.6 (value fraction of fibers $V = 10\%$, crack location $x/L = 0.1$)	37
<u>Numerical Result :</u>		
Figure.4.7	First three Non-dimensional frequencies of the non-cracked composite beam as a function of the angle of fibers α . Values of V: 0.02	42

Figure.4.8	First three Non-dimensional frequencies of the non-cracked composite beam as a function of the angle of fibers α . Values of V: 0.10	43
Figure.4.9	First three Non-dimensional frequencies of the non-cracked composite beam as a function of the angle of fibers α . Values of V: 0.30	43
Figure.4.10	First three Non-dimensional frequencies of the non-cracked composite beam as a function of the angle of fibers α . Values of V: 0.75	44
Figure.4.11	Changes in the First Non-dimensional natural frequencies of the cracked composite beam as a function of the angle of fibers α for several values of the crack depth $a/H = 0.2, 0.4$ and 0.6 (value fraction of fibers $V = 10\%$, crack location $x/L = 0.1$)	46
Figure.4.12	Changes in the Second Non-dimensional natural frequencies of the cracked composite beam as a function of the angle of fibers α for several values of the crack depth $a/H = 0.2, 0.4$ and 0.6 (value fraction of fibers $V = 10\%$, crack location $x/L = 0.1$)	46
Figure.4.13	First, Second and Third mode shapes of non-cracked composite beam	47
Figure.4.14	First mode shapes of cracked composite beam for $x=0.1L$ and relative cracked depth (rcd) = 0.2, 0.4, 0.6	47
Figure.4.15	Second mode shapes of cracked composite beam for $x=0.1L$ and relative cracked depth (rcd) = 0.2, 0.4, 0.6	48
Figure.4.16	Third mode shapes of cracked composite beam for $x=0.1L$ and relative cracked depth (rcd) = 0.2, 0.4, 0.6	48
Figure.4.17	The First Non-dimensional natural frequencies of the cracked composite beam as a function of volume fraction of fiber V for several values of the crack depth $a/H = 0.0, 0.2, 0.4$ and 0.6 (the angle of fiber $\alpha = 0$ degree, crack location $x/L = 0.1$)	50
Figure.4.18	The second non-dimensional natural frequencies of the cracked composite beam as a function of volume fraction of fiber V for several values of the crack depth $a/H = 0.0, 0.2, 0.4$ and 0.6 (the angle of fibers $\alpha = 0$ degree, crack location $x/L = 0.1$)	51
Figure.4.19	Relative changes in the first non-dimensional frequency ratios for different crack depth of the cracked composite beam	53

Figure.4.20	Relative changes in the second non-dimensional frequency ratios for different crack depth of the cracked composite beam	53
Figure.4.21	The first non-dimensional natural frequencies as a function of fiber orientation for the cases of three cracks located differently, as indicated $a/H=0.2$ and $V=0.1$	54
Figure.4.22	The second non-dimensional natural frequencies as a function of fiber orientation for the cases of three cracks located differently, as indicated $a/H=0.2$ and $V=0.1$	55
Figure.4.23	The third non-dimensional natural frequencies as a function of fiber orientation for the cases of three cracks located differently, as indicated $a/H=0.2$ and $V=0.1$	55
Figure.4.24	Critical buckling load vs. relative crack depth for different crack location when angle of fiber = 0 degree	58
Figure.4.25	Critical buckling load vs. crack location for different relative crack depth when angle of fiber = 0 degree	58
Figure.4.26	Critical buckling load vs. relative crack depth for different crack location when angle of fiber = 90 degree	59
Figure.4.27	Critical buckling load vs. crack location for different relative crack depth when angle of fiber = 90 degree	59

LIST OF TABLES

Table No.		Pages
Table-4.1	Properties of the graphite fibre-reinforced polyamide composite	30
	<u>Convergence study :</u>	
Table-4.2	Convergence of non-dimensional free vibration frequencies of cracked composite beam for different angle of fibers	32
	<u>Comparison with previous study:</u>	
Table-4.3	Comparison of non-dimensional natural frequencies of the non-cracked composite beam as a function of the angle of fibers α , where Value of $V=0.10$ and 0.30	34
Table-4.4	Comparison of non-dimensional natural frequencies of the cracked composite beam as a function of the angle of fibers (α) for several values of the crack depth $a/H = 0.2, 0.4, 0.6$ (value fraction of fibers $V = 10\%$, crack location $x/L = 0.1$)	36
Table-4.5	Buckling loads of a non-cracked composite beam for angle of fiber = $0, 30, 60$ and 90 degree	38
	<u>Numerical Result :</u>	
Table-4.6	First three non-dimensional natural frequencies of the non-cracked composite beam as a function of the angle of fibers α , where Value of $V=0.02$	40
Table-4.7	First three non-dimensional natural frequencies of the non-cracked composite beam as a function of the angle of fibers α , where Value of $V=0.10$	41
Table-4.8	First three non-dimensional natural frequencies of the non-cracked composite beam as a function of the angle of fibers α , where Value of $V = 0.30$	41
Table-4.9	First three non-dimensional natural frequencies of the non-cracked composite beam as a function of the angle of fibers α , where Value of $V=75$	42

Table-4.10	First Non-dimensional natural frequencies of the cracked composite beam as a function of the angle of fibers α for several values of the crack depth $a/H = 0.2, 0.4$ and 0.6 (value fraction of fibers $V = 10\%$, crack location $x/L = 0.1$)	45
Table-4.11	Second Non-dimensional natural frequencies of the cracked composite beam as a function of the angle of fibers α for several values of the crack depth $a/H = 0.2, 0.4$ and 0.6 (value fraction of fibers $V = 10\%$, crack location $x/L = 0.1$)	45
Table-4.12	First non-dimensional natural frequencies of the cracked composite beam as a function of value fraction of fibers V for several values of the crack depth $a/H = 0.0, 0.2, 0.4$ and 0.6 (the angle of fibers $\alpha = 0$ degree, crack location $x/L = 0.1$)	49
Table-4.13	Second non-dimensional natural frequencies of the cracked composite beam as a function of value fraction of fibers V for several values of the crack depth $a/H = 0.0, 0.2, 0.4$ and 0.6 (the angle of fibers $\alpha = 0$ degree, crack location $x/L = 0.1$)	50
Table-4.14	First non-dimensional frequency ratios for different crack depth	52
Table-4.15	Second non-dimensional frequency ratios for different crack depth	52
Table-4.16	Buckling loads for different crack locations for a composite cracked beam for angle of fiber $= 0, 30, 60$ and 90 degrees	57

LIST OF SYMBOLS

The principal symbols used in this thesis are presented for easy reference. A symbol is used for different meaning depending on the context and defined in the text as they occur.

English

Notation	Description
A	Cross-sectional area of the element
a/H	Crack depth
α	Angle of the fiber
C^0	Flexibility matrix of the non-cracked element
C_{ovl}	Overall stiffness matrix of the cracked element
B	Width of the composite beam
F_{ij}	Correction Function for Crack
G_s	Strain energy release rate
H	Height of the composite beam
I	Moment of inertia
K_{Crack}	Crack beam element stiffness matrix
$[K_e]$	Stiffness matrix due to bending

$[K_g]$	Geometric matrix
M_e	Element mass matrix
$K_I, K_{II} \text{ \& } K_{III}$	Stress intensity factors
L	Length of the composite beam
l_1	Crack location
$P(t)$	Periodic axial force
P_{cr}	Buckling load
q	Vector
ρ	Mass Density of the beam
S_{11}	Material property
$[T]$	Transformation matrix of the crack beam element
U	Strain energy
ω	Natural frequency
ω_n	Non-dimensional natural frequency
Y_j	Correction function for crack
ζ	Functions of the elastic constants

1.1 Introduction

Composites as structural material are being used in aerospace, military and civilian applications because of their tailor made properties. The ability of these materials to be designed to suit the specific needs for different structures makes them highly desirable. Improvement in design, materials and manufacturing technology enhance the application of composite structures. The suitability of a particular composite material depends on the nature of applications and needs. The technology has been explored extensively for aerospace and civil engineering applications, which require high strength and stiffness to weight ratio materials.

Preventing failure of composite material systems has been an important issue in engineering design. Composites are prone to damages like transverse cracking, fiber breakage, delamination, matrix cracking and fiber-matrix debonding when subjected to service conditions. The two types of physical failures that occur in composite structures and interact in complex manner are interlaminar and interlaminar failures. Interlaminar failure is manifest in micro-mechanical components of the lamina such as fiber breakage, matrix cracking, and debonding of the fiber-matrix interface. Generally, aircraft structures made of fiber reinforces composite materials are designed such that the fibers carry the bulk of the applied load. Interlaminar failure such as delamination refers to debonding of adjacent lamina. The possibility that interlaminar and interlaminar failure occur in structural components is considered a design limit, and establishes restrictions on the usage of full potential of composites.

Similar to isotropic materials, composite materials are subjected to various types of damage, mostly cracks and delamination. The crack in a composite structure may reduce the structural stiffness and strength, redistribute the load in a way that the structural failure is delayed, or may lead to structural collapse. Therefore, crack is not necessarily the ultimate structural failure, but rather it is the part of the failure process which may ultimately lead to loss of structural integrity.

As one of the failure modes for the fiber-reinforced composites, crack initiation and propagation have long been an important topic in composite and fracture mechanics communities. During operation, all structures are subjected to degenerative effects that may cause initiation of structural defects such as cracks which, as time progresses, lead to the catastrophic failure or breakdown of the structure. Thus, the importance of inspection in the quality assurance of manufactured products is well understood. Several methods, such as non-destructive tests, can be used to monitor the condition of a structure. It is clear that new reliable and inexpensive methods to monitor structural defects such as cracks should be explored. These variations, in turn, affect the static and dynamic behavior of the whole structure considerably. In some cases this can lead to failure, unless cracks are detected early enough. To ensure the safe, reliable and operational life of structures, it is of high importance to know if their members are free of cracks and, should they be present, to assess their extent. The procedures that are often used for detection are called direct procedures such as ultrasonic, X-rays, etc. However, these methods have proven to be inoperative and unsuitable in some particular cases, since they require expensive and minutely detailed inspections. To avoid these disadvantages, researchers have focused on more efficient procedures in crack detection based on the changes of modal parameters likes natural frequencies, mode shapes and modal damping values that the crack introduces.

Cracks or other defects in a structural element influence its dynamical behaviour and change its stiffness and damping properties. Consequently, the natural frequencies and mode shapes of the structure contain information about the location and dimensions of the damage. Vibration analysis can be used to detect structural defects such as cracks, of any structure offer an effective, inexpensive and fast means of nondestructive testing. What types of changes occur in the vibration characteristics, how these changes can be detected and how the condition of the structure is interpreted has been the topic of several research studies in the past. The use of composite materials in various construction elements has increased substantially over the past few years.

Cracks found in structural elements have various causes. They may be fatigue cracks that take place under service conditions as a result of the limited fatigue strength. They may also be due to mechanical defects, as in the case of turbine blades of jet turbine engines. In these engines the cracks are caused by sand and small stones sucked from the surface of the runway. Another group involves cracks which are inside the material: they are created as a result of manufacturing processes.

In this thesis **Chapter 2** presents the review of literature confining to the scope of the study. The analysis of vibration and buckling of cracked composite beam have been briefly addressed in this chapter. The **Chapter 3** presents some information about the theoretical background of composite beam and the mathematical formulation for the analysis of cracked composite beam using finite elements method. The elastic stiffness, the mass and geometric stiffness matrices for the non-cracked and cracked elements has been formulated. The computer program implementation of the theoretical formulations has been briefly described with the help of a flow chart. In **Chapter 4**, convergence study, comparison with previous study and numerical results

has been presented to validate the formulation of the proposed method. The **Chapter 5** concludes the present investigation. An account of possible scope of extension to the present study has been appended to the concluding remarks. Some important publications and books referred during the present investigation have been listed in the **References**.

1.2 Scope of the present Investigation

The main aim of this thesis is to work out a composite beam finite element with a non-propagating one-edge open crack. It has been assumed that the crack changes only the stiffness of the element whereas the mass of the element is unchanged. For theoretical modeling of cracked composite beam dimensions, crack locations, crack depth and material properties is specified. In this work an “overall additional flexibility matrix”, instead of the “local additional flexibility matrix” is added to the flexibility matrix of the corresponding non-cracked composite beam element to obtain the total flexibility matrix, and therefore the stiffness matrix in the line with the other researchers. By using the present model the following effects due to the crack of the cantilever composite beam have been analyzed.

- (1) The influence of the volume fraction of fibers, magnitude, location of the crack, angle of fibers upon the bending natural frequencies of the cantilever cracked composite beam.
- (2) The effects of above parameters on buckling analysis of cracked composite beam.

The present results are compared with previous studies and the new results are obtained in the MATLAB environment.

2.1 Introduction

The widespread use of composite structures in aerospace applications has stimulated many researchers to study various aspects of their structural behaviour. These materials are particularly widely used in situations where a large strength-to-weight ratio is required. Similarly to isotropic materials, composite materials are subjected to various types of damage, mostly cracks and delamination. These result in local changes of the stiffness of elements for such materials and consequently their dynamic characteristics are altered. This problem is well understood in case of constructing elements made of isotropic materials, while data concerning the influence of fatigue cracks on the dynamics of composite elements are scarce in the available literature.

Cracks occurring in structural elements are responsible for local stiffness variations, which in consequence affect their dynamic characteristics. This problem has been a subject of many papers, but only a few papers have been devoted to the changes in the dynamic characteristics of composite constructional elements. In the present investigation an attempt has been made to the reviews on composite cracked beam in the context of the present work and discussions are limited to the following area of analysis.

2.2 Review on vibration of cracked composite beam

A local flexibility will reduce the stiffness of a structural member, thus reducing its natural frequency. For small crack depths the change (decrease) in natural frequency is proportional to the square of the crack depth ratio.

Nikpour & Dimarogonas (1988) presented the local compliance matrix for unidirectional composite materials. They have shown that the interlocking deflection modes are enhanced as a function of the degree of anisotropy in composites.

Nikpour (1990) studied the effect of cracks upon buckling of an edge notched column for isotropic and anisotropic composites. He indicated that the instability increases with the column slenderness and the crack length. In addition he has shown that the material anisotropy conspicuously reduces the load carrying capacity of an externally cracked member.

Ostachowicz & Krawczuk (1991) presented a method of analysis of the effect of two open cracks upon the frequencies of the natural flexural vibrations in a cantilever beam. Two types of cracks were considered: double-sided, occurring in the case of cyclic loadings, and single-sided, which in principle occur as a result of fluctuating loadings. It was also assumed that the cracks occur in the first mode of fracture: i.e., the opening mode. An algorithm and a numerical example were included.

Manivasagam & Chandrasekaran (1992) presented results of experimental investigations on the reduction of the fundamental frequency of layered composite materials with damage in the form of cracks.

Krawczuk (1994) formulated a new beam finite element with a single non-propagating one-edge open crack located in its mid-length for the static and dynamic analysis of cracked composite beam-like structures. The element includes two degrees of freedom at each of the three nodes: a transverse deflection and an independent rotation respectively. He presented the exemplary numerical calculations illustrating variations in the static deformations and a fundamental bending natural frequency of a composite cantilever beam caused by a single crack.

Krawczuk & Ostachowicz (1995) investigated eigen frequencies of a cantilever beam made from graphite-fiber reinforced polyimide, with a transverse on-edge non-propagating open crack. Two models of the beam were presented. In the first model the crack was modeled by a massless substitute spring Castigliano's theorem. The second model was based on the finite element method. The undamaged parts of the beam were modeled by beam finite elements with three nodes and three degrees of freedom at the node. The damaged part of the beam was replaced by the cracked beam finite element with degrees of freedom identical to those of the non-cracked done. The effects of various parameters the crack location, the crack depth, the volume fraction of fibers and the fibers orientation upon the changes of the natural frequencies of the beam were studied. Computation results indicated that the decrease of the natural frequencies not only depends on the position of the crack and its depth as in the case of isotropic material but also that these changes strongly depend on the volume fraction of the fiibers and the angle of the fibers of the composite material.

Ghoneam (1995) presented the dynamic characteristics laminated composite beams (LCB) with various fiber orientations and different boundary fixations and discussed in the absence and presence of cracks. A mathematical model was developed, and experimental analysis was utilized to study the effects of different crack depths and locations, boundary conditions, and various code numbers of laminates on the dynamic characteristics of CLCB. The analysis showed good agreement between experimental and theoretical results.

Dimarogonas (1996) reported a comprehensive review of the vibration of cracked structures. This author covered a wide variety of areas that included cracked beams, coupled systems, flexible rotors, shafts, turbine rotors and blades, pipes and shells, empirical diagnoses of machinery cracks, and bars and plates with a significant collection of references.

Krawczuk, Ostachowicz & Zak (1997) presented a model and an algorithm for creation of the characteristic matrices of a composite beam with a single transverse fatigue crack. The element developed had been applied in analyzing the influence of the crack parameters (position and relative depth) and the material parameters (relative volume and fibre angle) on changes in the first four transverse natural frequencies of the composite beam made from unidirectional composite material.

Hamada (1998) studied the variations in the eigen-nature of cracked composite beams due to different crack depths and locations. A numerical and experimental investigation has been made. The numerical finite element technique was utilized to compute the eigen pairs of laminated composite beams through several state of cracks. The model was based on elastic-plastic fracture mechanics techniques in order to consider the crack tip plasticity in the analysis. The model has been applied to investigate the effects of state of crack, lamina code number, boundary condition on the dynamic behavior of composite beams.

Zak, Krawczuk & Ostachowicz (2000) developed the work models of a finite delaminated beam element and delaminated plate element. They carried out an extensive experimental investigation to establish changes in the first three bending natural frequencies due to delaminations. The subsequent results of the numerical calculations were consistent the results of the experimental investigations.

Banerjee (2001) derived exact expressions for the frequency equation and mode shapes of composite Timoshenko beams with cantilever end conditions in explicit analytical form by using symbolic computation. The effect of material coupling between the bending and torsional modes of deformation together with the effects of shear deformation and rotatory inertia is taken into

account when formulating the theory. The expressions for the mode shapes were also derived in explicit form using symbolic computation.

Wang & Inmana (2002) investigated the free vibration of a cantilever beam, made of unidirectional fiber-reinforced composite, of high aspect ratio and with an open edge crack is. The beam model is based on the classical lamination theory; the crack modeled with the local flexibility method such that the cantilever beam could be replaced with two intact beams with the crack as the additional boundary condition. It was demonstrated that changes of eigen-frequencies and corresponding mode shapes depend on not only the crack location and ratio, but also the material properties (fiber orientation, fiber volume fraction).

Kisa (2003), investigated the effects of cracks on the dynamical characteristics of a cantilever composite beam, made of graphite fibre-reinforced polyamide. The finite element and the component-mode synthesis methods were used to model the problem. The cantilever composite beam divided into several components from the crack sections. The effects of the location and depth of the cracks, and the volume fraction and orientation of the fibers on the natural frequencies and mode shapes of the beam with transverse non-propagating open cracks, were explored. The results of the study led to conclusions that, presented method was adequate for the vibration analysis of cracked cantilever composite beams, and by using the drop in the natural frequencies and the change in the mode shapes, the presence and nature of cracks in a structure can be detected.

Wang, Inmana & Farrar (2004) investigated the coupled bending and torsional vibration of a fiber-reinforced composite cantilever with an edge surface crack. The model was based on linear fracture mechanics, the Castigliano's theorem and classical lamination theory. The crack was

modeled with a local flexibility matrix such that the cantilever beam was replaced with two intact beams with the crack as the additional boundary condition. The coupling of bending and torsion can result from either the material properties or the surface crack.

Lu & Law (2009) studied such effect from multiple cracks in a finite element in the dynamic analysis and local damage identification. The finite beam element was formulated using the composite element method with a one-member–one-element configuration with cracks where the interaction effect between cracks in the same element was automatically included. The accuracy and convergence speed of the proposed model in computation were compared with existing models and experimental results. The parameter of the crack model was found needing adjustment with the use of the proposed model.

2.3 Review on buckling analysis of composite cracked beam

In the present investigation an attempt has been made to the reviews on composite beam in the context of the present work. This problem has been a subject of many papers, but only a few papers have been devoted to the changes in the static characteristics of cracked composite elements.

Przemieniecki and **Purdy** (1968) presented the general analysis for large deflections of frame structures using concept of discrete element idealizations. They were presented the results for deflections of a six-bay truss and buckling of columns with either constant axial load or gravity loading.

Ozturk & Sabuncu (2005) examined the static and dynamic stabilities of a laminated composite cantilever beam having linear translation spring and torsional spring as elastic supports subjected

to periodic axial loading. The beam was assumed to be an Euler beam and modeled by using the finite element method. The model was considered to have symmetric and asymmetric lay-ups. The effects of the variation of cross-section in one direction, the ratio of length to thickness, orientation angle, static and dynamic load parameters, stiffness of elastic supports having linear translation spring and torsional spring, and position of the elastic support on stability were examined. In addition, the obtained results of the fundamental natural frequency and critical buckling load parameters were compared with the results of other investigators in existing literature.

Goyal & Kapania (2008) performed a stability analysis of laminated beam structures subject to sub-tangential loading, a combination of conservative and non-conservative tangential follower loads, using the dynamic criterion. These loads were characterized using a non-conservativeness loading parameter. This parameter allows them to study the effect of the level of load conservativeness on the stability of laminated beams. The element tangent stiffness and mass matrices were obtained using analytical integration through the dynamic version of the principle of virtual work for laminated composites.

Akbulut, Gundogdu & Sengul (2010) studied on the theoretical prediction of buckling loads for symmetric angle-ply and cross-ply laminated flat composite columns, consisting of two portions of different widths connected by fillets. They obtained the buckling loads of the column under axial compression for the following end conditions: simply supported, simply-clamped, clamped-clamped, and clamped free.

Discussions are limited to the cracked composite beam for area of buckling analysis.

Nikpour (1990) studied the buckling of an edge-notched beam for isotropic and anisotropic composites. The local compliance due to the presence of cracks in an anisotropic medium was formulated as a function of the crack-tip stress intensity factors and the elastic constants of the material. The effect of reducing rigidity on the load-carrying capacity and the post-buckling behavior of the beam was discussed.

Yang & Chen (2008) presented a theoretical investigation in free vibration and elastic buckling of beams made of functionally graded materials (FGMs) containing open edge cracks by using Bernoulli–Euler beam theory and the rotational spring model. Analytical solutions of the natural frequencies, critical buckling load, and the corresponding mode shapes were obtained for cracked FGM beams with clamped–free, hinged–hinged, and clamped–clamped end supports. A detailed parametric study was conducted to show the influences of the location and total number of cracks, material properties, slenderness ratio, and end supports on the flexural vibration and buckling characteristics of cracked FGM beams.

Karaagac, Ozturk & Sabuncu (2011) investigated the effects of a single-edge crack and its locations on the buckling loads, natural frequencies and dynamic stability of circular curved beams using the finite element method, based on energy approach. This study consists of three stages, namely static stability (buckling) analysis, vibration analysis and dynamic stability analysis. The governing matrix equations were derived from the standard and cracked curved beam elements combined with the local flexibility concept. Results showed that the reductions in buckling load and natural frequency depend not only on the crack depth and crack position, but also on the related mode shape. Analyses also showed that the crack effect on the dynamic stability of the considered curved beam was quite limited.

3.1 Introduction

Structures are weakened by cracks. When the crack size increases in course of time, the structure becomes weaker than its previous condition. Finally, the structure may breakdown due to a minute crack. The basic configuration of the problem investigated here is a composite beam of any boundary condition with a transverse one-edge non-propagating open crack. However, a typical cracked cantilever composite beam, which has tremendous applications in aerospace structures and high-speed turbine machinery, is considered.

The following aspects of the crack greatly influence the dynamic response of the structure.

- i. The position of a crack in a cracked composite beam
- ii. The depth of crack in a cracked composite beam
- iii. The angle of fibers in a cracked composite beam
- iv. The volume fraction of fibers in a cracked composite beam

3.2 The Methodology

The governing equations for the vibration analysis of the composite beam with an open one-edge transverse crack are developed. An additional flexibility matrix is added to the flexibility matrix of the corresponding composite beam element to obtain the total flexibility matrix and therefore the stiffness matrix is obtained by Krawczuk & Ostachowicz (1995).

The assumptions made in the analysis are:

- i. The analysis is linear. This implies constitutive relations in generalized Hook's law for the materials are linear.
- ii. The Euler–Bernoulli beam model is assumed.
- iii. The damping has not been considered in this study.
- iv. The crack is assumed to be an open crack and have uniform depth 'a'.

3.3 Governing Equation

The differential equation of the bending of a beam with a mid-plane symmetry ($B_{ij} = 0$) so that there is no bending-stretching coupling and no transverse shear deformation ($\epsilon_{xz} = 0$) is given by;

$$IS_{11} \frac{d^4 \omega}{dx^4} = q \quad x \quad (1)$$

It can easily be shown that under these conditions if the beam involves only a one layer, isotropic material, then $IS_{11} = EI = Ebh^3/12$ and for a beam of rectangular cross-section Poisson's ratio effects are ignored in beam theory, which is in the line with Vinson & Sierakowski (1991).

In Equation 1, it is seen that the imposed static load is written as a force per unit length. For dynamic loading, if Alembert's Principle are used then one can add a term to Equation.1 equal to the product mass and acceleration per unit length. In that case Equation.1 becomes

$$IS_{11} \frac{d^4 \omega(x,t)}{dx^4} = q(x,t) - \rho A \frac{\partial^2 \omega(x,t)}{\partial x^2} \quad (2)$$

where ω and q both become functions of time as well as space, and derivatives therefore become partial derivatives, ρ is the mass density of the beam material, and here A is the beam cross-sectional area. In the above, $q(x, t)$ is now the spatially varying time-dependent forcing function

causing the dynamic response, and could be anything from a harmonic oscillation to an intense one-time impact.

For a composite beam in which different lamina have differing mass densities, then in the above equations use, for a beam of rectangular cross-section,

$$\rho A = \rho b h = \sum_{k=1}^N \rho b (h_k - h_{k-1}) \quad (3)$$

However, natural frequencies for the beam occur as functions of the material properties and the geometry and hence are not affected by the forcing functions; therefore, for this study let $q(x, t)$ be zero.

Thus, the natural vibration equation of a mid-plane symmetrical composite beam is given by;

$$I S_{11} \frac{d^4 \omega(x, t)}{dx^4} + \rho A \frac{\partial^2 \omega(x, t)}{\partial t^2} = 0 \quad (4)$$

It is handy to know the natural frequencies of beams for various practical boundary conditions in order to insure that no recurring forcing functions are close to any of the natural frequencies, because that would result almost certainly in a structural failure. In each case below, the natural frequency in radians/unit time are given as

$$\omega_n = \alpha^2 \left(\frac{I S_{11}}{\rho A L^4} \right)^{1/2} \quad (5)$$

where α^2 is the co-efficient, which value is catalogued by Warburton, Young and Felgar and once ω_n is known then the natural frequency in cycles per second (Hertz) is given by $f_n = \omega_n / 2\pi$, which is in the line with Vinson & Sierakowski (1991).

3.4 Mathematical Model

The model chosen is a cantilever composite beam of uniform cross-section A, having an open-edge transverse crack of depth 'a' at position ' l_1 '. The width, length and height of the beam are B, L and H, respectively in Figure.3.1. The angle between the fibers and the axis of the beam is ' α '.

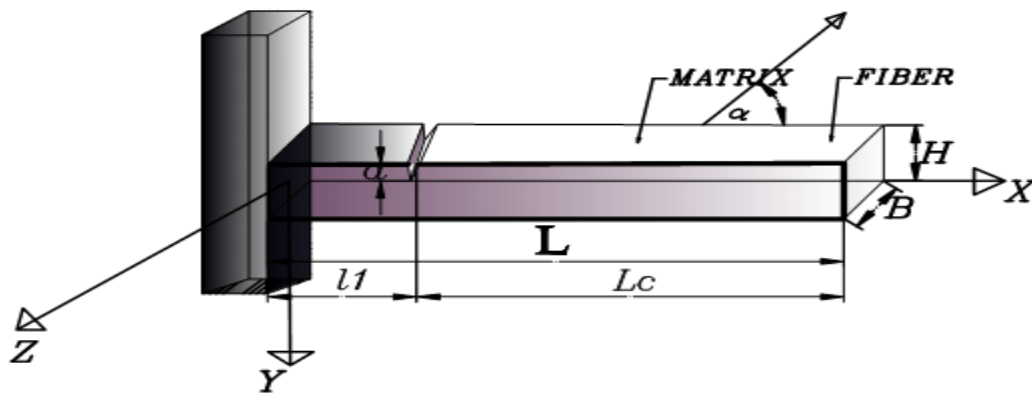


Figure.3.1 Schematic diagram cantilever composite beam with a crack

3.4.1 Buckling analysis studies

Mass and stiffness matrices of each beam element are used to form global mass and stiffness matrices. The dynamic response of a beam for a conservative system can be formulated by means of Lagrange's equation of motion in which the external forces are expressed in terms of time-dependent potentials and then performing the required operations the entire system leads to the governing matrix equation of motion

$$M \ddot{q} + K_e - P(t) K_g \quad q = 0 \quad (6)$$

where 'q' is the vector of degree of freedoms. M , K_e and K_g are the mass, elastic stiffness and geometric stiffness matrices of the beam. The periodic axial force $P(t) = P_o + P_t \cos \Omega t$, where Ω is the disturbing frequency, the static and time dependent components of the load can be represented as a fraction of the fundamental static buckling load P_{cr} hence putting $P(t) = \alpha P_{cr} + \beta P_{cr} \cos \Omega t$.

In this analysis, the computed static buckling load of the composite beam is considered the reference load. Further the above equation reduces to other problems as follows.

- i. Free vibration with $\alpha = 0$, $\beta = 0$ and $\omega = \Omega/2$ the natural frequency

$$K_e - \omega^2 M \quad q = 0 \quad (7.a)$$

- ii. Static stability with $\alpha = 1$, $\beta = 0$, $\Omega = 0$

$$K_e - P_{cr} K_g \quad q = 0 \quad (7.b)$$

3.4.2 Derivation of Element Matrices

In the present analysis three nodes composite beam element with three degree of freedom (the axial displacement, transverse displacement and the independent rotation) per node is considered. The characteristic matrices of the composite beam element are computed on the basis of the model proposed by Oral (1991). The stiffness and mass matrices are developed from the procedure given by Krawczuk & Ostachowicz (1995).

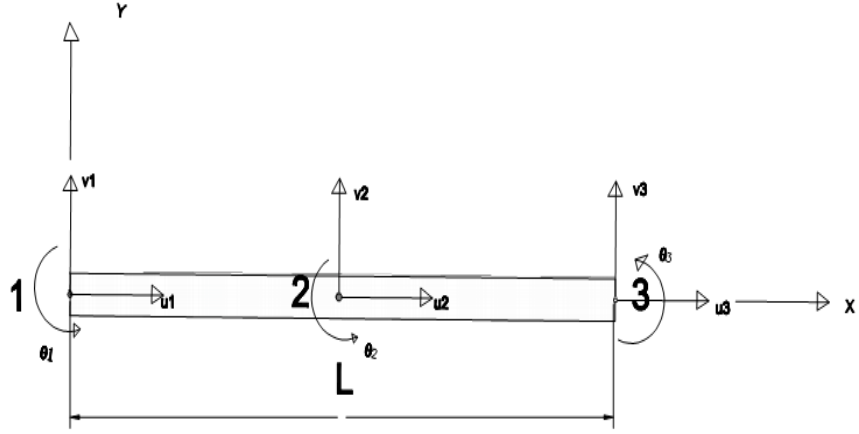


Figure.3.2 Nodal displacements in the element coordinate system

The linear strain can be described in terms of displacements as

$$\varepsilon = B \delta \quad (8)$$

where displacement vector in the element reference beam is given as

$$\delta = \begin{bmatrix} u_1 \\ v_1 \\ \theta_1 \\ u_2 \\ v_2 \\ \theta_2 \\ u_3 \\ v_3 \\ \theta_3 \end{bmatrix}$$

3.4.2.1 Stress-Strain matrix

$$D = \begin{bmatrix} S_{11} & S_{13} \\ S_{13} & S_{33} \end{bmatrix} \quad (9)$$

where the element of the matrix D are expressed in Appendix A.

Following standard procedures the element stiffness matrix, mass matrix and geometrical stiffness matrix can be expressed as follows:

3.4.2.2 Element stiffness matrix

Element stiffness matrix for a three-nodes composite beam element with three degrees of freedom $\delta = (u, v, \theta)$ at each node, for the case of bending in the x, y plan, are given in the line Krawczuk & Ostachowicz (1995) as follows:

$$K_e = IS_{11} \int_0^L [B]^T D B dv \quad (10)$$

where $[B] = \frac{\partial}{\partial x^2} N$ = strain displacement matrix, $[N]$ = shape function matrix and

$K_e = [k_{ij}]_{9 \times 9}$ where $[k_{ij}]_{9 \times 9} = (i, j = 1, \dots, 9)$ are

$$k_{11} = k_{77} = 7BHS_{11}/3L,$$

$$k_{12} = k_{21} = k_{78} = k_{87} = 7BHS_{13}/3L,$$

$$k_{12} = k_{21} = k_{78} = k_{87} = 7BHS_{13}/3L,$$

$$k_{13} = k_{31} = (-k_{79}) = (-k_{97}) = BHS_{13}/2,$$

$$(-k_{14}) = (-k_{41}) = k_{47} = k_{74} = 8BHS_{11}/3L,$$

$$-k_{15} = (-k_{51}) = (-k_{42}) = (-k_{24}) = (-k_{48}) = (-k_{84}) = (-k_{57}) = (-k_{75}) = 8BHS_{13}/3L,$$

$$k_{16} = k_{61} = (-k_{34}) = (-k_{43}) = k_{49} = k_{94} = (-k_{67}) = (-k_{76}) = 2BHS_{13}/3,$$

$$k_{17} = k_{71} = BHS_{11}/3L,$$

$$k_{18} = k_{81} = k_{27} = k_{72} = BHS_{13}/3L,$$

$$k_{73} = k_{37} = (-k_{19}) = (-k_{91}) = BHS_{13}/6,$$

$$k_{22} = k_{88} = 7BHS_{33}/3L,$$

$$k_{23} = k_{32} = (-k_{89}) = (-k_{98}) = BHS_{33}/2,$$

$$(-k_{25}) = (-k_{52}) = (-k_{58}) = (-k_{85}) = 8BHS_{33}/3L,$$

$$k_{26} = k_{62} = k_{59} = k_{95} = (-k_{53}) = (-k_{35}) = (-k_{86}) = (-k_{68}) = 2BHS_{33}/3,$$

$$k_{28} = k_{82} = BHS_{33}/3L,$$

$$k_{38} = k_{83} = (-k_{29}) = (-k_{92}) = BHS_{33}/6,$$

$$k_{45} = k_{54} = 16BHS_{13}/3L,$$

$$k_{44} = 16BHS_{11}/3L,$$

$$k_{55} = 16BHS_{33}/3L,$$

$$k_{33} = k_{99} = BH \{ (7S_{11}H^2/36L) + (S_{33}L/9) \},$$

$$k_{36} = k_{63} = k_{69} = k_{96} = BH \{ (-2S_{11}H^2/9L) + (S_{33}L/9) \},$$

$$k_{39} = k_{93} = BH \{ (S_{11}H^2/36L) - (S_{33}L/18) \},$$

$$k_{66} = BH \{ (4S_{11}H^2/9L) + (4S_{33}L/9) \},$$

$$k_{46} = k_{56} = 0$$

where B is the width of the element, H is the height of the element and L denotes the length of the element. S_{11} , S_{13} and S_{33} are the stress-strain constants

3.4.2.3 Generalized element mass matrix

Element mass matrix of the non-cracked composite beam element is given in the line Krawczuk & Ostachowicz (1995) as

$$M_e = \rho \int_v [N]^T N dv \quad (11)$$

$M_e = [m_{ij}]_{9 \times 9}$ where $[m_{ij}]_{9 \times 9} = (i, j = 1, \dots, 9)$ are

$$M_e = \rho BHL \begin{bmatrix} \frac{2}{15} & 0 & 0 & \frac{2}{15} & 0 & 0 & -\frac{1}{30} & 0 & 0 \\ 0 & \frac{2}{15} & \frac{L}{180} & 0 & \frac{1}{15} & \frac{-L}{90} & 0 & \frac{-1}{30} & \frac{L}{180} \\ 0 & \frac{L}{180} & \frac{L^2}{1890} + \frac{H^2}{90} & 0 & 0 & \frac{-L^2}{945} + \frac{H^2}{180} & 0 & \frac{-L}{180} & \frac{L^2}{1890} - \frac{H^2}{90} \\ \frac{2}{15} & 0 & 0 & \frac{8}{15} & 0 & 0 & \frac{1}{15} & 0 & 0 \\ 0 & \frac{1}{15} & 0 & 0 & \frac{8}{15} & 0 & 0 & \frac{1}{15} & 0 \\ 0 & \frac{-L}{90} & \frac{-L^2}{945} + \frac{H^2}{180} & 0 & 0 & \frac{2L^2}{1890} + \frac{2H^2}{90} & 0 & \frac{L}{90} & \frac{-L^2}{945} + \frac{H^2}{180} \\ -\frac{1}{30} & 0 & 0 & \frac{1}{15} & 0 & 0 & \frac{2}{15} & 0 & 0 \\ 0 & \frac{-1}{30} & \frac{-L}{180} & 0 & \frac{1}{15} & \frac{-L}{90} & 0 & \frac{2}{15} & \frac{-L}{180} \\ 0 & \frac{L}{180} & \frac{L^2}{1890} - \frac{H^2}{90} & 0 & 0 & \frac{-L^2}{945} + \frac{H^2}{180} & 0 & \frac{-L}{180} & \frac{L^2}{1890} + \frac{H^2}{90} \end{bmatrix}$$

where ρ is the mass density of the element, B is the width of the element, H is the height of the element and L denotes the length of the element.

3.4.2.4 Geometrical stiffness matrix

Geometrical stiffness matrix of the composite beam element is given in the line Przemieniecki and Purdy (1968) as

$$K_g = T \int_0^L N'^T N' dx \quad (12)$$

$$K_g = \frac{T}{30L} \begin{bmatrix} 36 & -36 & -36 & 3L & -3L & -36 & 36 & -36 & 3L \\ -36 & 36 & 36 & -3L & 3L & 36 & -36 & 36 & -3L \\ -36 & 36 & 36 & -3L & 3L & 36 & -36 & 36 & -3L \\ 3L & -3L & -3L & 4L^2 & -4L^2 & -3L & 3L & -3L & -L^2 \\ -3L & 3L & 3L & -4L^2 & 4L^2 & 3L & -3L & 3L & L^2 \\ -36 & 36 & 36 & -3L & 3L & 36 & -36 & 36 & -3L \\ 36 & -36 & -36 & 3L & -3L & -36 & -36 & -36 & -3L \\ -36 & 36 & 36 & -3L & 3L & 36 & -36 & 36 & -3L \\ 3L & -3L & -3L & -L^2 & L^2 & -3L & -3L & -3L & 4L^2 \end{bmatrix}$$

where T is an initial tension of the element and L denotes the length of the element.

3.4.2.5 Stiffness matrix for cracked composite beam element

The most convenient method to obtain the stiffness matrix of a cracked composite beam element is to obtain the total flexibility matrix first and then take inverse of it. The total flexibility matrix of the cracked element includes two parts. The first part is the additional flexibility matrix due to the existence of crack, which leads to energy release and additional deformation of the structure. The second part is original flexibility matrix of the non-cracked composite beam.

a) Elements of the overall additional flexibility matrix C_{ovl}

Let B = breadth of the composite beam element

H = depth of the composite beam element

L = Length of the composite beam element

l_1 = Distance between the left hand side end node i and crack location

A = Cross-sectional area of the composite beam

I = Moment of inertia

According to the St. Venant's principle, the stress field is influenced only in the region near to the crack. The additional strain energy due to crack leads to flexibility coefficients expressed by stress intensity factors derived by means of Castigliano's theorem in the linear elastic range. In this study, the bending-stretching effect due to mid-plane asymmetry induced by the cracks is neglected. The compliance coefficients c_{ij} induced by crack are derived from the strain energy release rate. The strain energy (U) of the beam due to crack and can be expressed as

$$U = \int_A G_s dA \quad (13)$$

Where G_s = the strain energy release rate,

A = the area of the crack section,

$$G_s = \frac{1}{2} \left(D_1 \sum_{i=1}^N K_{Ii}^2 + D_{12} \sum_{i=1}^N K_{Ii} K_{IIi} + D_2 \sum_{i=1}^N K_{IIi}^2 + D_3 \sum_{i=1}^N K_{IIIi}^2 \right) \quad (14)$$

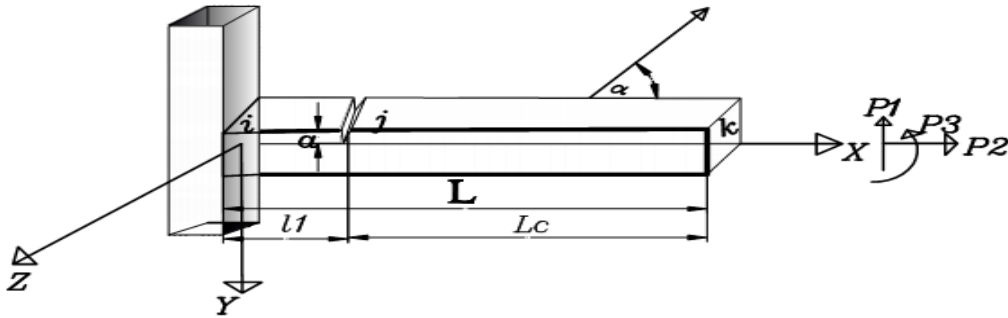


Figure.3.3 A typical cracked composite beam element subjected to shearing force and bending moment

where K_I , K_{II} & K_{III} = Stress intensity factors for fracture modes of opening, sliding and tearing type cracks and the coefficients D_1 , D_{12} , D_2 & D_3 are given by the following relations

$$D_1 = -0.5Q_{11}I_m \frac{s_1 + s_2}{s_1 s_2}$$

$$D_{12} = Q_{12}I_m(s_1 s_2)$$

$$D_1 = -0.5Q_{11}I_m \frac{s_1 + s_2}{s_1 s_2}$$

$$D_3 = 0.5 \frac{Q_{44}Q_{55}}{Q_{44}Q_{55}} \quad (15)$$

The expression for the stress intensity factors from earlier studies is given by,

$$K_{ij} = \sigma_i \frac{\pi a Y_j(\zeta)}{H} F_{ij} \frac{a}{H} \quad (16)$$

The correction factors $Y_j(\zeta)$ and $F_{ji}(a/H)$ arise from the lack of symmetry and the deformation at the free edges of the beam compared with an infinite plate containing a crack. These factors are non-dimensional functions of the relative depth of the crack ($a = \frac{a}{H}$). The correction functions $Y_j(\zeta)$ and $F_{ji}(a/H)$ ($j = I, II$, $i = 1, 6$) are taken from the line Krawczuk & Ostachowicz (1995)

$$F_{I1} = F_{I4} = F_I = \frac{\tan \gamma}{\gamma} [0.752 + 2.02 \frac{a}{H} + 0.37(1 - \sin \gamma)^3 / \cos \gamma] \quad (17.a)$$

$$F_{I2} = F_{I3} = F_{I5} = F_{I6} = F_{II} \frac{\tan \gamma}{\gamma} [0.923 + 0.199(1 - \sin \gamma)^4 / \cos \gamma] \quad (17.b)$$

$$F_{II2} = F_{II5} = F_{III} = 1.122 - 0.561 \frac{a}{H} + 0.85(\frac{a}{H})^2 + 0.18(\frac{a}{H})^3 / \sqrt{1 - \frac{a}{H}} \quad (17.c)$$

$$Y_I \zeta = 1 + 0.1 \zeta - 1 - 0.016(\zeta - 1)^2 + 0.002(\zeta - 1)^3, \quad Y_{II} \zeta = 1 \quad (18)$$

where $\gamma = \pi a/2H$

The dimensionless parameters λ and ζ are defined as functions of the elastic constants by

$$\lambda = \frac{E_{22}}{E_{11}}, \quad \zeta = \frac{\overline{E_{22}E_{11}}}{2G_{12}} - \frac{\overline{\nu_{12}\nu_{21}}}{\nu_{12}\nu_{21}} \quad (19)$$

Applying the Castigliano's theorem yields the overall additional flexibility matrix of the element

C^1 due to the crack in the form

$$C^1 = c_{ij}^1, \quad i = 1, 6; j = 1, 6 \quad \text{and} \quad c_{ij}^1 = c_{ji}^1 \quad (20)$$

with the terms of the matrix C^1 being given by

$$c_{11}^1 = -c_{14}^1 = c_{44}^1 = \frac{2D_1\pi}{B} \int_0^a a (F_{II}Y_I)^2 da \quad (20.a)$$

$$c_{12}^1 = c_{15}^1 = -c_{24}^1 = -c_{45}^1 = -\frac{6D_1\pi L}{BH} \int_0^a a F_{II}F_{III}Y_I^2 da - \frac{D_{12}\pi}{B} \int_0^a a F_{II}F_{III}Y_I da \quad (20.b)$$

$$c_{13}^1 = -c_{16}^1 = -c_{34}^1 = -c_{46}^1 = \frac{12D_1\pi}{BH} \int_0^a a F_{II}F_{III}Y_I^2 da \quad (20.c)$$

$$c_{22}^1 = c_{55}^1 = \frac{18D_1\pi L^2}{BH^2} \int_0^a a (F_{II}Y_I)^2 da + \frac{2D_2\pi}{B} \int_0^a a (F_{III})^2 da + \frac{6D_{12}\pi L}{BH} \int_0^a a F_{II}F_{III}Y_I da \quad (20.d)$$

$$c_{23}^1 = c_{35}^1 = -c_{26}^1 = -c_{56}^1 = -\frac{36D_1\pi L^2}{BH^2} \int_0^a a (F_{II}Y_I)^2 da - \frac{6D_{12}\pi}{BH} \int_0^a a F_{II}F_{III}Y_I da \quad (20.e)$$

$$c_{25}^1 = \frac{18D_1\pi L^2}{BH^2} \int_0^a a (F_{II}Y_I)^2 da + \frac{2D_2\pi}{B} \int_0^a a (F_{III})^2 da \quad (20.f)$$

$$c_{33}^1 = -c_{36}^1 = c_{66}^1 = \frac{72D_1\pi}{BH^2} \int_0^a a (F_{II}Y_I)^2 da \quad (20.g)$$

where $\bar{a} = a/H$ and $d\bar{a} = da/H$

Now the overall stiffness matrix $C^1 = C_{ovl}$ is given by

$$C_{ovl} = \begin{matrix} c_{11}^1 & c_{12}^1 & c_{13}^1 & c_{14}^1 & c_{15}^1 & c_{16}^1 \\ c_{21}^1 & c_{22}^1 & c_{23}^1 & c_{24}^1 & c_{25}^1 & c_{26}^1 \\ c_{31}^1 & c_{32}^1 & c_{33}^1 & c_{34}^1 & c_{35}^1 & c_{36}^1 \\ c_{41}^1 & c_{42}^1 & c_{43}^1 & c_{44}^1 & c_{45}^1 & c_{46}^1 \\ c_{51}^1 & c_{52}^1 & c_{53}^1 & c_{54}^1 & c_{55}^1 & c_{56}^1 \\ c_{61}^1 & c_{62}^1 & c_{63}^1 & c_{64}^1 & c_{65}^1 & c_{66}^1 \end{matrix} \quad (21)$$

b) Flexibility matrix for the $C^0 = C_{Intact}$ composite beam

The flexibility matrix of the non-cracked element C^0 is determined by the force-displacement equation, i.e.

$$P_i = K_{e,ij} q_j \quad i = 1,9, \quad j = 1,9 \quad (22)$$

where P = the column matrix of the dependent nodal forces

q = the column matrix of the nodal displacements

and K_e denotes the stiffness matrix of the non-cracked element.

$$q_i = K_{e,ij}^{-1} P_j \quad (23)$$

Finally, the flexibility matrix of the non-cracked element $C^0 = C_{intact}$ is in the form

$$C^0_{k,k} = K_{e,ij}^{-1}, \quad i = 1,2,3,7,8,9, \quad j = 1,2,3,7,8,9, \quad k = 1,6 \quad (24)$$

c) Total flexibility matrix C_{total} of the cracked composite beam element

$$C_{total} = C_{intact} + C_{ovl} \quad (25)$$

d) Stiffness matrix K_{Crack} of a cracked composite beam element:

From equilibrium condition is plotted in Figure.3.4.

$$[U_1 \ V_1 \ \theta_1 \ U_2 \ V_2 \ \theta_2 \ U_3 \ V_3 \ \theta_3]^T = [T](U_2 \ V_2 \ \theta_2)^T \quad (26)$$

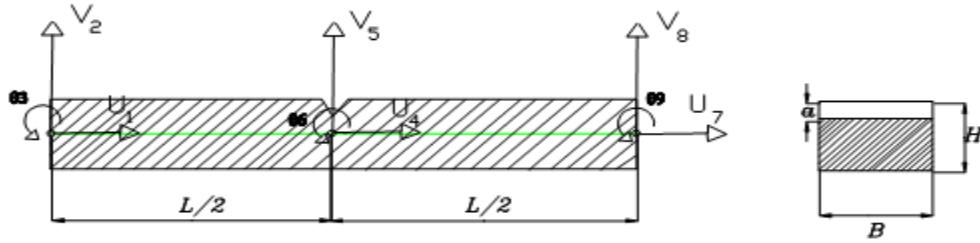


Figure.3.4 Geometry of a finite composite beam element with an open crack

The matrix of transformation $[T]$ is calculated by using the equation of overall equilibrium for element forces P_i ($i = 1,9$) and S_i ($i = 1,6$). The final form of this matrix is

$$[T]^t = \begin{bmatrix} 1 & 0 & 0 & 0 & 0 & 0 \\ 0 & 1 & 0 & 0 & 0 & 0 \\ 0 & 0 & 1 & 0 & 0 & 0 \\ -1 & 0 & 0 & -1 & 0 & 0 \\ 0 & -1 & 0 & 0 & -1 & 0 \\ 0 & L/2 & -1 & 0 & L/2 & -1 \\ 0 & 0 & 0 & 1 & 0 & 0 \\ 0 & 0 & 0 & 0 & 1 & 0 \\ 0 & 0 & 0 & 0 & 0 & 1 \end{bmatrix} \quad (27)$$

Hence the stiffness matrix K_{Crack} of a cracked beam element can be obtained as

$$K_{Crack} = TC_{total}^{-1}T^t \quad (28)$$

3.5 Computational procedure for a cracked composite beam

A computer program is developed to perform all the necessary computations in MATLAB environment. In the initialization phase, geometry and material parameters are specified. For example for a Euler–Bernoulli composite beam model with localized crack, material parameters like modulus of elasticity, the modulus of rigidity, the Poisson ratio and the mass density of the composite beam material and geometric parameters like dimensions of the composite beam, also the specifications of the damage like size of the crack, location of the crack and extent of crack are supplied as input data to the computer program. The beam is divided into n number of elements and $n+1$ number of nodes. The elements of the mass matrix, elastic stiffness matrix and geometric stiffness matrix are formulated according to above expression and are obtained the non-dimensional natural frequencies and buckling load for non-cracked and cracked composite beam element. The program uses the MATLAB function, “Gauss Quadrature” to carry out the integration part. Element matrices are assembled to obtain the global matrices. Boundary conditions are imposed by elimination method. For Euler–Bernoulli composite beam with fixed-free end conditions the first three rows and columns of the global matrices are eliminated to obtain the reduced matrices. The non-dimensional natural frequencies are calculated by solving the Eigen value problems in eq. 5. The built in MATLAB function “eig” is used to calculate the eigen values, eigenvectors and mode shape diagram.

3.5.1 Flow Chart of the program

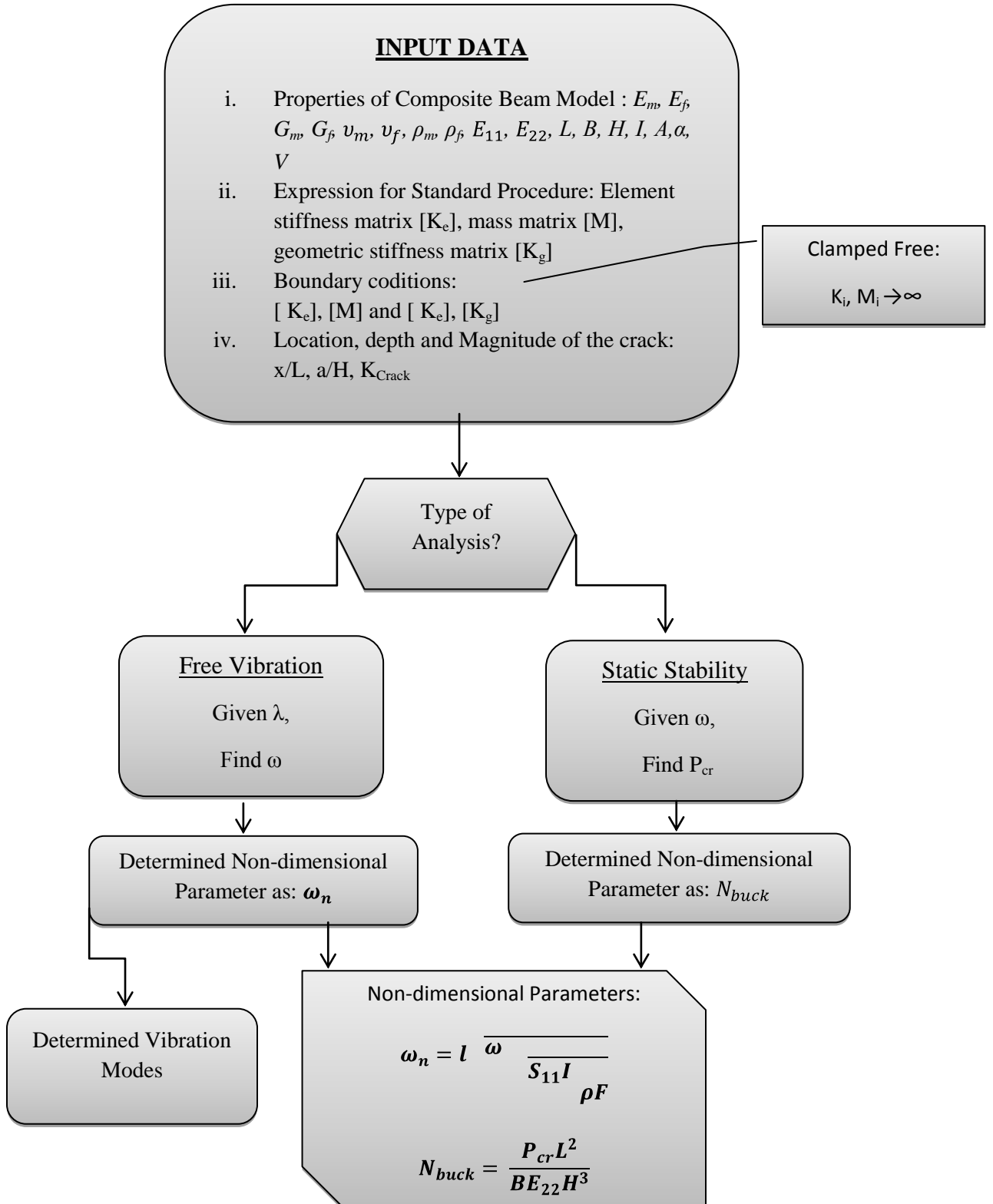


Fig.3.5 Flowchart utilized in the Static stability and Free vibration analyses

Effect of an open edge transverse crack on various parameters of a composite beam like vibration and buckling are studied and compared with previously studied results. The formulation is then validated and extended for other problems.

4.1 Introduction

In order to check the accuracy of the present analysis, the case considered in Krawczuk & Ostachowicz (1995) is adopted here. The beam assumed to be made of unidirectional graphite fiber-reinforced polyamide. The geometrical characteristics and material properties of the beam are chosen as the same of those used in Krawczuk & Ostachowicz (1995). The material properties of the graphite fiber-reinforced polyamide composite, in terms of fibers and matrix, is identified by the indices f and m, respectively, are in Table-4.1

Table-4.1 Properties of the graphite fibre-reinforced polyamide composite

Modulus of Elasticity	E_m	2.756 GPa
	E_f	275.6 GPa
Modulus of Rigidity	G_m	1.036 GPa
	G_f	114.8GPa
Poisson's Ratio	ν_m	0.33
	ν_f	0.2
Mass density	ρ_m	1600 kg/m ³
	ρ_f	1900 kg/m ³

The geometrical characteristics, the length (L), height (H) and width (B) of the composite beam, are taken as 1.0 m, 0.025 m and 0.05m respectively.

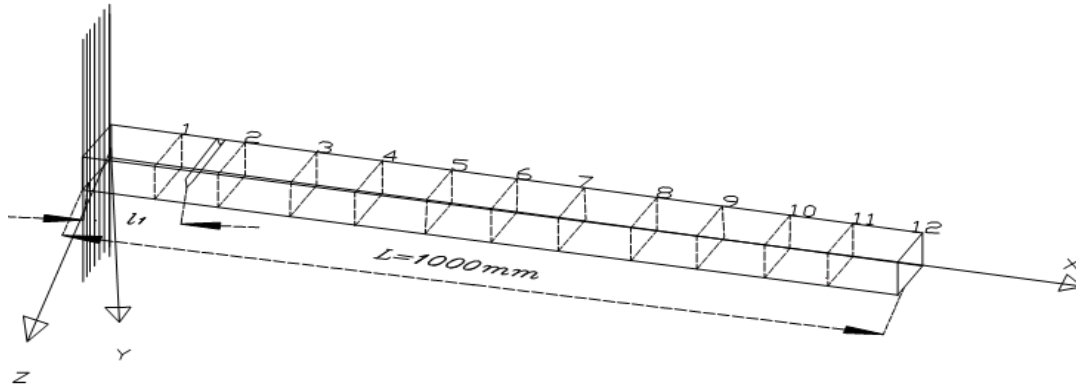


Figure.4.1 Geometry of cantilever cracked composite beam with 12 elements

In this chapter, the results of vibration and buckling analysis of composite beam structure with or without crack are presented using the formulation given in Chapter-3. Each of the cracked composite beam problems is presented separately for the following studies:

- I. Convergence Studies
- II. Comparison with Previous Studies
- III. Numerical Result
 - A. Vibration and Buckling Analysis of results of composite beam with single crack
 - B. Vibration Analysis of results of composite beam with multiple cracks

4.2 Convergence Study

The convergence study is carried out for the free vibration of cracked composite beam and omitted here for sake of brevity. Based on this study, a mesh of 12 elements shows good convergence of numerical solutions for free vibration of cracked composite beam, which is shown in Fig.4.2.

Table-4.2 Convergence of non-dimensional free vibration frequencies of cracked composite beam for different angle of fibers

$V = 0.1$, $a/H = 0.2$, $E_m = 2.756$; $E_f = 275.6$; $\nu_f = .2$; $G_m = 1.036$; $G_f = 114.8$; $\rho_m = 1600$; $\rho_f = 1900$;

$$\text{Non dimensional frequency, } \omega_n \alpha = l \sqrt{\frac{\omega \alpha = 0}{S_{11} I \rho F}}$$

Mesh Division	Non dimensional frequencies for different angle of fibers "α"(degrees)		
	α = 0	α = 15	α = 30
2 elements	1.5982	1.6703	1.7125
4 elements	1.6815	1.7255	1.7732
8 elements	1.6995	1.7257	1.7748
12 elements	1.7055	1.7245	1.7743
Krawczuk & Ostachowicz (1995)	1.7055	1.7245	1.7743

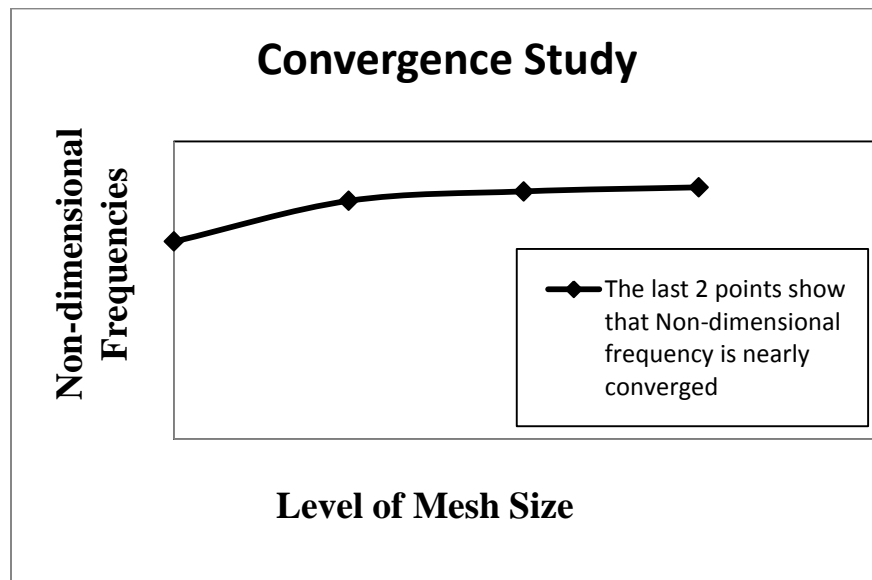


Figure.4.2 The convergence of non-dimensional free vibration frequencies of cracked composite beam for angle of fibers "α = 0" (degrees)

4.3 Comparison with Previous Studies

Quantitative results on the effects of various parameters on the vibration and buckling analysis of cracked composite are presented.

4.3.1 Vibration analysis studies

The presented method has been applied for the free vibration analysis of a non-cracked and cracked composite cantilever beam. Free vibration analysis of a cantilever cracked composite beam has been examined by Krawczuk & Ostachowicz (1995) using finite element method (FEM). In this study the results obtained with present element are compared with the results of Krawczuk & Ostachowicz. Throughout this investigation, 12 elements are used in modeling the cracked composite beam. In addition, the three lowest eigen-frequencies for various values of the angle of the fiber (α) and the volume fraction of fibers (V) are determined and given in Table-4.3 and Fig. 4.3, 4.4. In Figure.4.5 and 4.6 the changes of the two first natural frequencies of the beam due to the crack as functions of the angle of fibers (α) are compared with the results of Krawczuk & Ostachowicz(1995). As seen from the tables agreements are good.

The non-dimensional natural frequencies are normalized according to the following relation;

$$\omega_n(\alpha) = l \sqrt{\frac{S_{11} I}{\rho F}} \omega(\alpha = 0) \quad (29)$$

where $\omega_n(\alpha)$ denotes the natural frequency of the beam computed for the fibers angle $\alpha = 0$ degree.

Table-4.3: Comparison of First three Non-dimensional natural frequencies of the non-cracked composite beam as a function of the angle of fibers α , where Value of $V=0.10$ and 0.30

Angle of Fibers (degrees)		Present Analysis			Krawczuk & Ostachowicz (1995)		
	Volume of Fraction V	1 st Non- dimension al Nat. freq	2 nd Non- dimension al Nat. freq	3 rd Non- dimension al Nat. freq	1 st Non- dimension al Nat. freq	2 nd Non- dimension al Nat. freq	3 rd Non- dimension al Nat. freq
0	0.10	1.8798	4.6566	7.6681	1.85145	4.52827	7.71888
15		1.8243	4.5300	7.4841	1.81768	4.51477	7.51418
30		1.6655	4.1530	6.9033	1.65453	4.12945	6.89687
45		1.4342	3.5854	5.9833	1.38995	3.53323	5.97735
60		1.2083	3.0230	5.0513	1.15370	3.01580	5.01780
75		1.0998	2.7514	4.5973	1.08133	2.74520	4.57040
90		1.0881	2.7205	4.5410	1.08007	2.71020	4.51710
0	0.30	1.8771	4.6113	7.5073	1.85145	4.52827	7.64894
15		1.8188	4.4873	7.3447	1.81768	4.44477	7.37372
30		1.6484	4.0982	6.7804	1.65453	4.02945	6.92680
45		1.3886	3.4682	5.7818	1.38995	3.43323	5.85710
60		1.1068	2.7684	4.6260	1.15370	2.71580	4.76640
75		0.948	2.3713	3.9632	1.08133	2.27052	4.04030
90		0.9307	2.3263	3.8831	1.08007	2.21720	3.97620

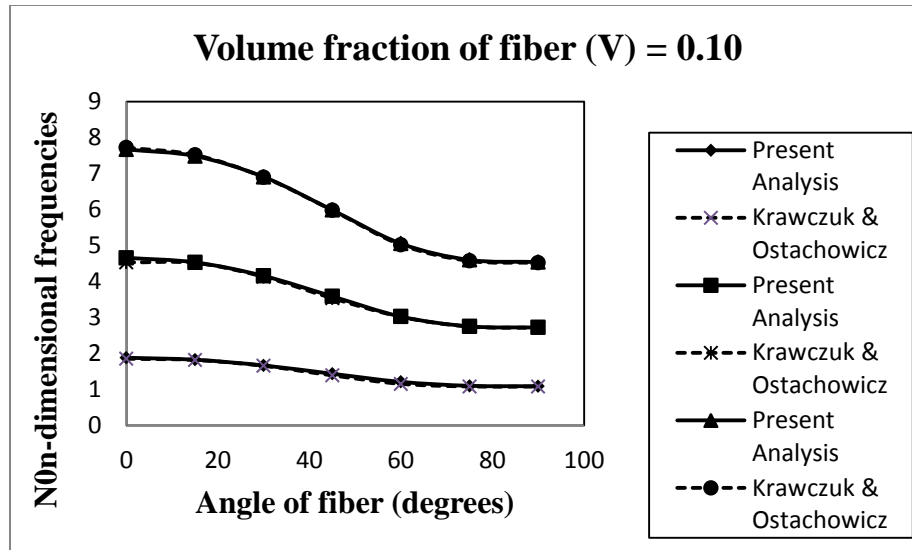


Figure.4.3 First three non-dimensional frequencies of the non-cracked composite beam as a function of the angle of fibers α . Values of V: 0.1

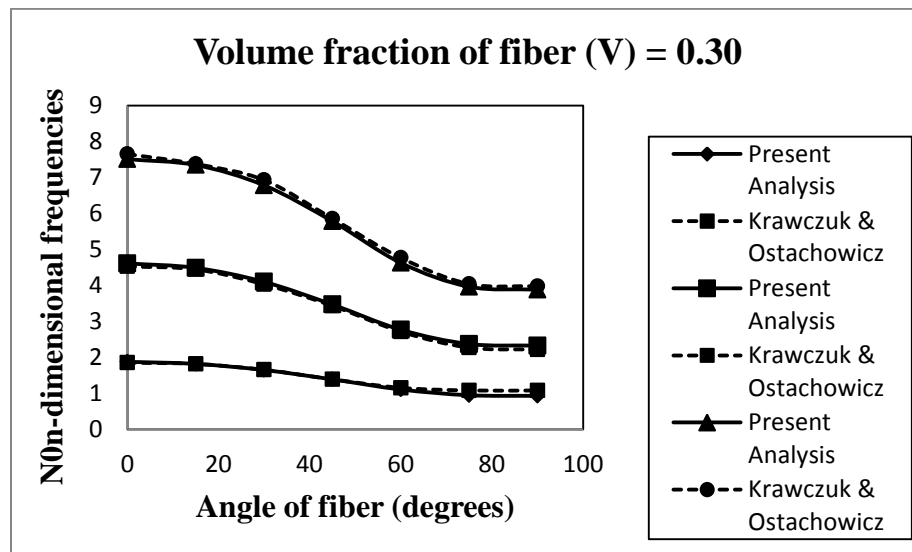


Figure.4.4 First three non-dimensional frequencies of the non-cracked composite beam as a function of the angle of fibers α . Values of V: 0.30

Table-4.4 Comparison of Non-dimensional natural frequencies of the cracked composite beam as a function of the angle of fibers (α) for several values of the crack depth $a/H = 0.2, 0.4, 0.6$ (value fraction of fibers $V = 10\%$, crack location $x/L = 0.1$)

Angle of Fibers (degrees)	Relative Cracked depth (a/H)	Present Analysis		Krawczuk & Ostachowicz (1995)	
		1 st Non- dimensional Nat. freq	2 nd Non- dimensional Nat. freq	1 st Non- dimensional Nat. freq	2 nd Non- dimensional Nat. freq
0	0.2	1.7070	4.5477	1.7100	4.5400
15		1.7260	4.5656	1.7260	4.5600
30		1.7755	4.6064	1.7705	4.6000
45		1.8337	4.6489	1.8297	4.6400
60		1.8738	4.6771	1.8728	4.6700
75		1.8875	4.6858	1.8805	4.6808
90		1.8886	4.6898	1.8806	4.6820
0	0.4	1.4110	4.4495	1.4150	4.4315
15		1.4428	4.6590	1.4458	4.4500
30		1.5359	4.5075	1.5452	4.5000
45		1.6723	4.5654	1.6753	4.5700
60		1.7939	4.6232	1.7940	4.6232
75		1.8432	4.6492	1.8332	4.6492
90		1.8479	4.6497	1.8409	4.6497
0	0.6	1.2216	4.2150	1.1316	4.2210
15		1.2530	4.2414	1.1930	4.2400
30		1.3484	4.3243	1.3184	4.3300
45		1.4996	4.4474	1.5004	4.4500
60		1.6511	4.5732	1.6523	4.5600
75		1.7189	4.6233	1.7189	4.6200
90		1.7256	4.6272	1.7356	4.6272

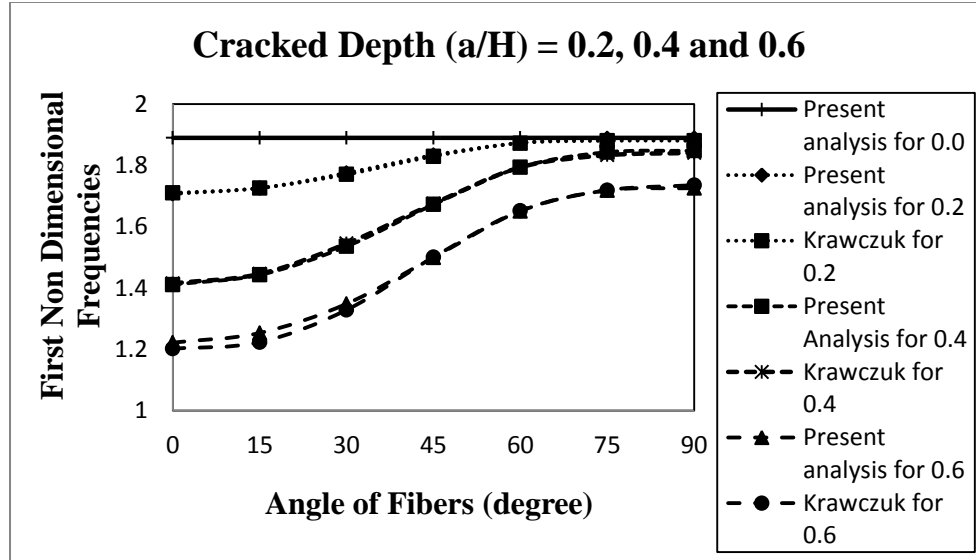


Figure.4.5 Changes in the First Non-dimensional natural frequencies of the cracked composite beam as a function of the angle of fibers α for several values of the crack depth $a/H = 0.0, 0.2, 0.4$ and 0.6 (value fraction of fibers $V = 10\%$, crack location $x/L = 0.1$)

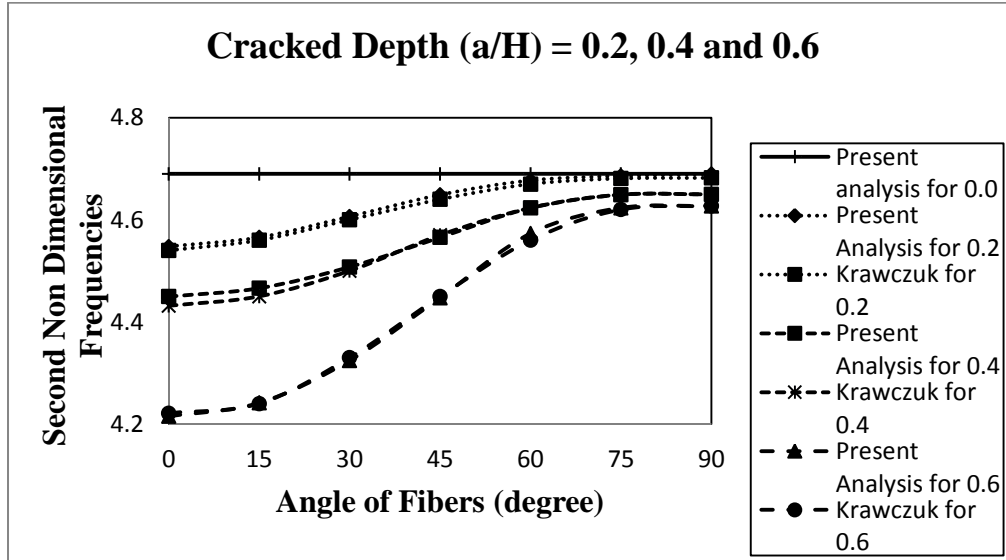


Figure 4.6 Changes in the second non-dimensional natural frequencies of the cracked composite beam as a function of the angle of fibers α for several values of the crack depth $a/H = 0.0, 0.2, 0.4$ and 0.6 (value fraction of fibers $V = 10\%$, crack location $x/L = 0.1$)

4.3.2 Buckling analysis studies

In this buckling analysis study, the results of non-cracked composite beam obtained with the present element are compared with the analytical results of Reddy (1997) and Ozturk & Sabuncu (2005). Table-4.5 shows the comparison of present results of buckling load with the results of Reddy (1997) and Ozturk & Sabuncu (2005) for various values of the angle of the fiber (α). As seen from the tables agreements are good.

The buckling loads are normalized according to the following relation;

$$N_{buck} = \frac{P_{cr}L^2}{BE_{22}H^3} \quad (30)$$

where N_{buck} denotes for the non-dimensional buckling load, P_{cr} denotes for the critical buckling load, L, B, H and E_{22} denote for the length, width, height and material property of the non-cracked composite beam.

Table-4.5: Buckling loads of a non-cracked composite beam for angle of fiber = 0, 30, 60 and 90 degree

Angle of fibers (degree)	Present FEM	Ozturk & Sabuncu (2005)	Reddy (1997)
0	4.9984	5.1404	5.14
30	1.6632	-	-
60	0.3891	-	-
90	0.2006	0.2056	0.205

4.4 Numerical Results

After obtaining the comparison with previous study and validating the formulation with the existing literatures, the results for non-dimensional natural frequencies of the non-cracked composite beam as a function of the angle of fibers (α) are presented. The changes of the two first natural frequencies of the beam due to the crack as functions of the angle of fibers (α) and volume fraction of fiber are analyzed and buckling analysis is carried out for free vibration of a composite beam with single crack for various crack positions and crack depths. Similarly, the three first natural frequencies of the composite beam due to the crack as functions of the angle of fibers (α) and volume fraction of fiber are analyzed for free vibration of a composite beam with multiple cracks for various crack positions. The beam assumed to be made of unidirectional graphite fiber-reinforced polyamide. The geometrical characteristics and the material properties of the graphite fiber-reinforced polyamide composite beam are chosen as the same of those used in Ozturk & Sabuncu (2005). The material properties of the graphite fiber-reinforced polyamide composite are

$$E_{11} = 129.207\text{GPa}, \quad E_{22} = 9.42512\text{GPa},$$

$$G_{12} = 5.15658\text{GPa}, \quad G_{13} = 4.3053\text{GPa}, \quad G_{23} = 2.5414\text{GPa},$$

$$\nu_{12} = \nu_{13} = \nu_{23} = 0.3$$

The geometrical characteristics, the length (L), height (H) and width (B) of the composite beam were chosen as 1.0m, .009525m and 0.0127m, respectively.

The crack is located at $x/L = 0.1, 0.2, 0.4, 0.6$ and 0.8 .

Relative crack depth (a/H) = $0.2, 0.4$ and 0.6

4.4.1 (A) Vibration analysis of results of composite beam with single crack

Firstly, the present method has been applied for the free vibration analysis of a non-cracked composite cantilever beam by using twelve elements FE model of the same length. The three lowest non-dimensional natural frequencies for various values of the angle of fibers (α) and the volume fraction of fibers (V) are determined and tabulated in Table 4.6, 4.7, 4.8 and 4.9. The results are also plotted in Figures 4.7 to 4.10. As the angle of the fiber increases from 0° to 90° , the non-dimensional natural frequency decreases. It is also found that the rate of decrease in non dimensional natural frequency with increase in volume fraction of fibers is more as the volume approaches approximately 45%.

Table-4.6 Numerical Result of First three non-dimensional natural frequencies of the non-cracked composite beam as a function of the angle of fibers α , where Value of V=0.02

Angle of fibers(degree)	Present analysis		
	1 st Non-dimensional Frequency	2 nd Non-dimensional Frequency	3 rd Non-dimensional Frequency
0	2.6780	6.2190	10.3191
15	2.6605	6.3681	10.2488
30	2.6286	6.1887	10.0580
45	2.5081	5.8617	9.7541
60	2.2001	5.0901	9.0700
75	1.8163	4.4184	8.1543
90	1.6045	4.0736	7.4392

Table-4.7 Numerical Result of First three Non-dimensional natural frequencies of the non-cracked composite beam as a function of the angle of fibers α , where Value of $V=0.1$

Angle of fibers(degree)	Present analysis		
	1 st Non-dimensional Frequency	2 nd Non-dimensional Frequency	3 rd Non-dimensional Frequency
0	2.4957	6.1828	10.1850
15	2.4674	6.1118	10.0653
30	2.3785	6.1887	9.6933
45	2.2201	5.8898	9.0445
60	1.9891	5.4987	8.1248
75	1.7186	4.9374	7.1049
90	1.5685	4.2808	6.5070

Table-4.8 Numerical Result of First three Non-dimensional natural frequencies of the non-cracked composite beam as a function of the angle of fibers α , where Value of $V=0.30$

Angle of fibers(degree)	Present analysis		
	1 st Non-dimensional Frequency	2 nd Non-dimensional Frequency	3 rd Non-dimensional Frequency
0	2.4929	6.1383	10.0266
15	2.4401	6.0128	9.8280
30	2.2873	5.6482	9.2407
45	2.0519	5.0821	8.2490
60	1.7649	4.3856	7.1315
75	1.4848	3.6997	6.1433
90	1.3486	3.3634	5.5950

Table-4.9 Numerical Result of first three Non-dimensional natural frequencies of the non-cracked composite beam as a function of the angle of fibers α , where Value of $V=0.75$

Angle of fibers(degree)	Present analysis		
	1 st Non-dimensional Frequency	2 nd Non-dimensional Frequency	3 rd Non-dimensional Frequency
0	2.4949	6.1707	10.1411
15	2.4561	6.0755	9.9854
30	2.3406	5.7925	9.5224
45	2.1519	5.3314	8.7553
60	1.8999	4.7187	7.7553
75	1.6244	4.0468	6.7182
90	1.4769	3.6835	6.1278

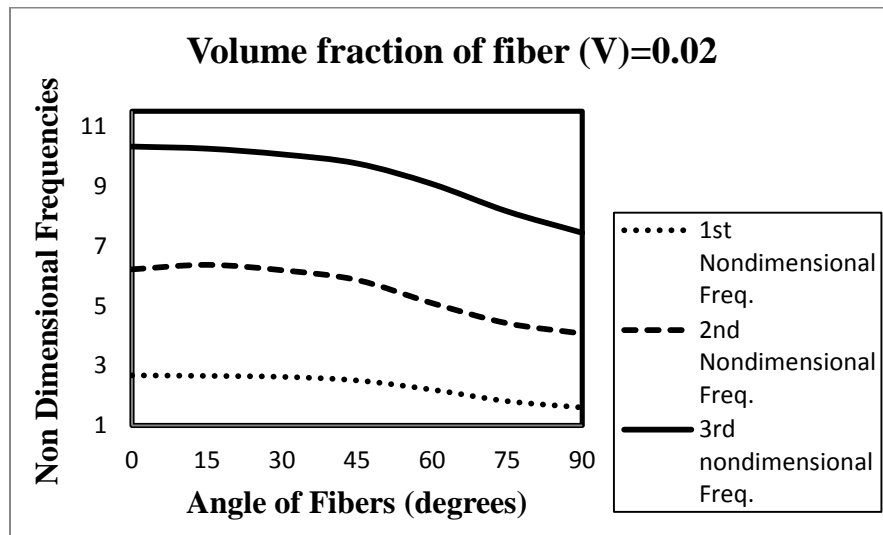


Figure 4.7 First three Non-dimensional frequencies of the non-cracked composite beam as a function of the angle of fibers α . Values of V : 0.02

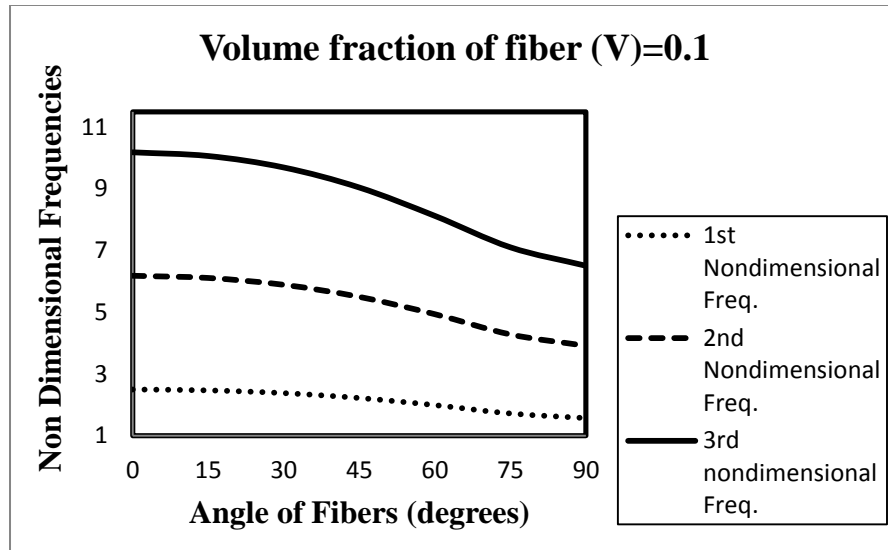


Figure 4.8 First three Non-dimensional frequencies of the non-cracked composite beam as a function of the angle of fibers α . Values of V : 0.10

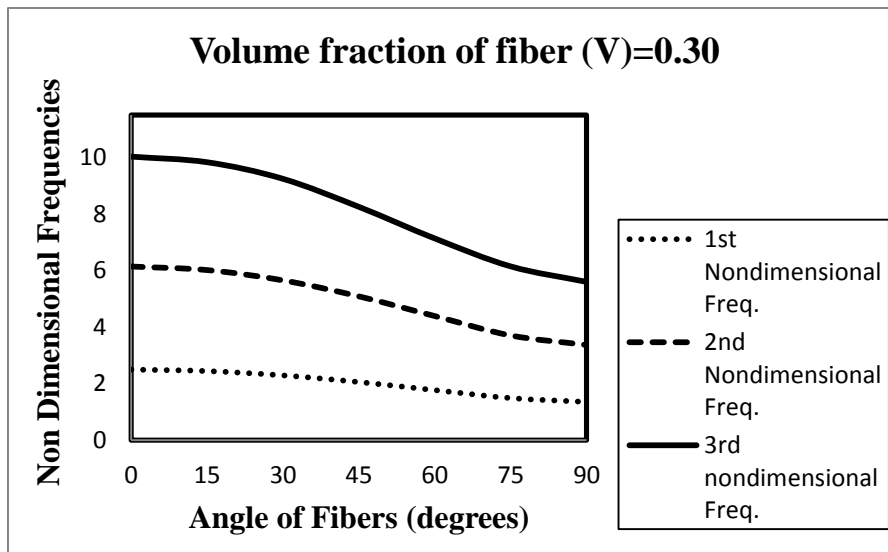


Figure 4.9 First three Non-dimensional frequencies of the non-cracked composite beam as a function of the angle of fibers α . Values of V : 0.30

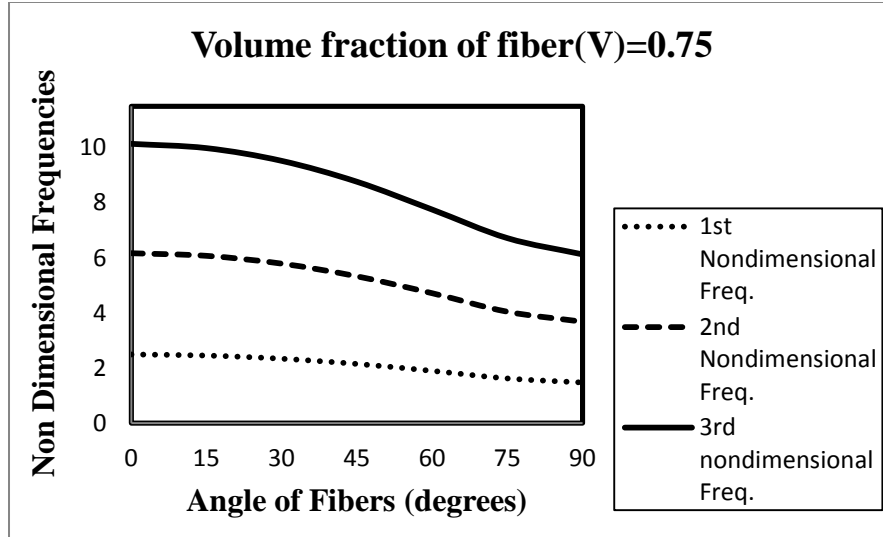


Figure 4.10 First three Non-dimensional frequencies of the non-cracked composite beam as a function of the angle of fibers α . Values of V : 0.75

Secondly, the non-dimensional natural frequencies and mode shapes of the cantilever composite beam having a transverse one-edge non-propagating open crack are analyzed. The calculations have been carried out for various values of the fiber angle (α), depth of the crack (a/H) and the fiber volume fraction ($V = 0.1$). The model of the composite beam contains eleven non-cracked beam elements and one element with a crack as shown in Figure 4.1. The crack was located at a distance $x = 0.1L$ (m) from the fixed end of the beam. The changes in the first two natural frequency of the cracked beam are given as a function of crack ratios (a/H) and the fiber orientations (α), which is tabulated in Table 4.10 and 4.1 and plotted in Figure 4.11 and 4.12. As seen in Figure 4.11, when the crack is perpendicular to the fiber direction, the decrease in the first natural frequencies are highest. When, the angle of fibers (α) increase the values of the natural frequencies also increase. The most difference in frequency occurs when the angle of fiber (α) is 0 degree. This is due to the fact that the flexibility of the composite beam due to crack is a function of the angle between the crack and the reinforcing fibers. It is noticeable that

decreases in the natural frequencies become more intensive with the growth of the depth of crack as seen in Figure 4.11 and 4.12.

Table-4.10 First Non-dimensional natural frequencies of the cracked composite beam as a function of the angle of fibers α for several values of the crack depth $a/H = 0.2, 0.4$ and 0.6 (value fraction of fibers $V = 10\%$, crack location $x/L = 0.1$)

crack position	Angle of fibers(degree)	Relative crack depth (a/h)		
		0.2	0.4	0.6
$x = 0.1L$	0	2.1348	1.6184	1.4667
	15	2.1674	1.6611	1.5062
	30	2.2552	1.7918	1.6279
	45	2.3652	2.005	1.8285
	60	2.4475	2.2334	2.0462
	75	2.4707	2.3502	2.158
	90	2.4719	2.3665	2.1736

Table-4.11 Second Non-dimensional natural frequencies of the cracked composite beam as a function of the angle of fibers α for several values of the crack depth $a/H = 0.2, 0.4$ and 0.6 (value fraction of fibers $V = 10\%$, crack location $x/L = 0.1$)

crack position	Angle of fibers(degree)	Relative crack depth (a/h)		
		0.2	0.4	0.6
$x = 0.1L$	0	5.8707	5.0340	3.9570
	15	5.931	5.1943	4.0078
	30	6.0789	5.4406	4.1638
	45	6.2307	5.6969	4.4199
	60	6.3201	5.9196	4.702
	75	6.3452	6.0772	4.8534
	90	6.3337	6.1704	4.8754

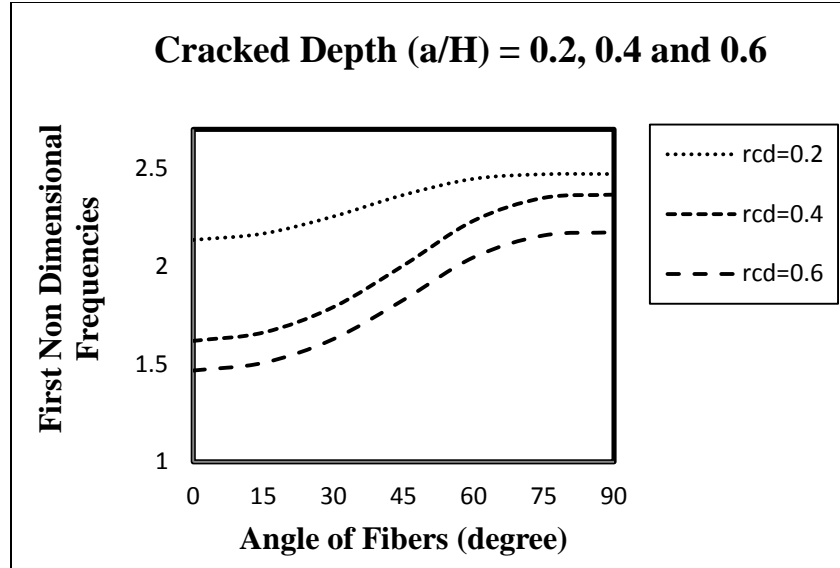


Figure 4.11 Changes in the First Non-dimensional natural frequencies of the cracked composite beam as a function of the angle of fibers α for several values of the crack depth $a/H = 0.2, 0.4$ and 0.6 (value fraction of fibers $V = 10\%$, crack location $x/L = 0.1$)

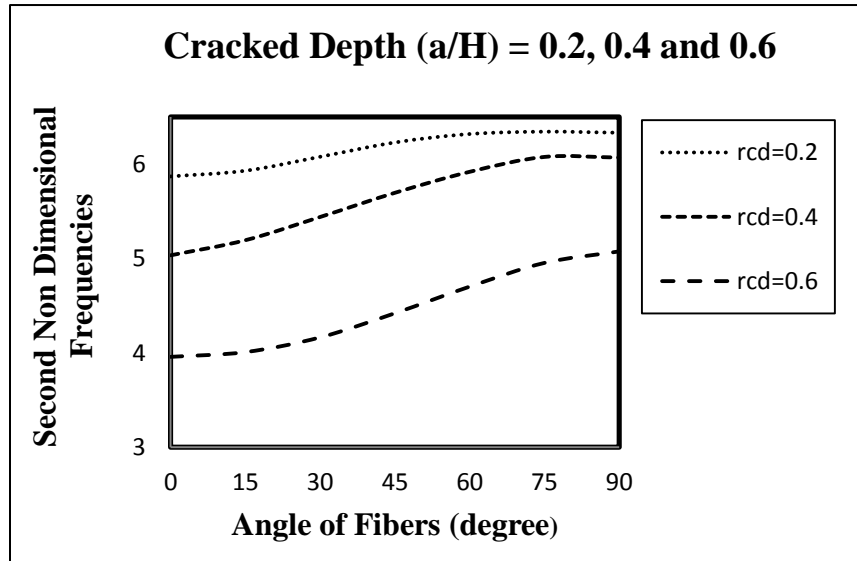


Figure 4.12 Changes in the First Non-dimensional natural frequencies of the cracked composite beam as a function of the angle of fibers α for several values of the crack depth $a/H = 0.2, 0.4$ and 0.6 (value fraction of fibers $V = 10\%$, crack location $x/L = 0.1$)

This conclusion is clearly seen from Figure 4.13, which illustrates the first three natural bending mode shapes of the non-cracked composite beam. This change of mode shapes can be used to detect the crack location as well as its magnitude for practical problems. The figures 4.14 to 4.16 show the mode shapes of vibration for the first three fundamental frequencies of a cracked beam with one-edge transverse crack at $0.1L$ for different crack depths.

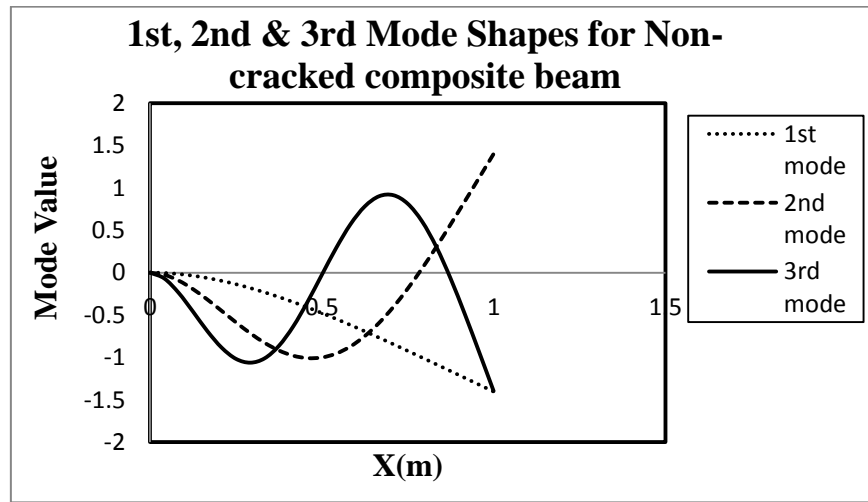


Figure 4.13 First, Second and Third mode shapes of non-cracked composite beam

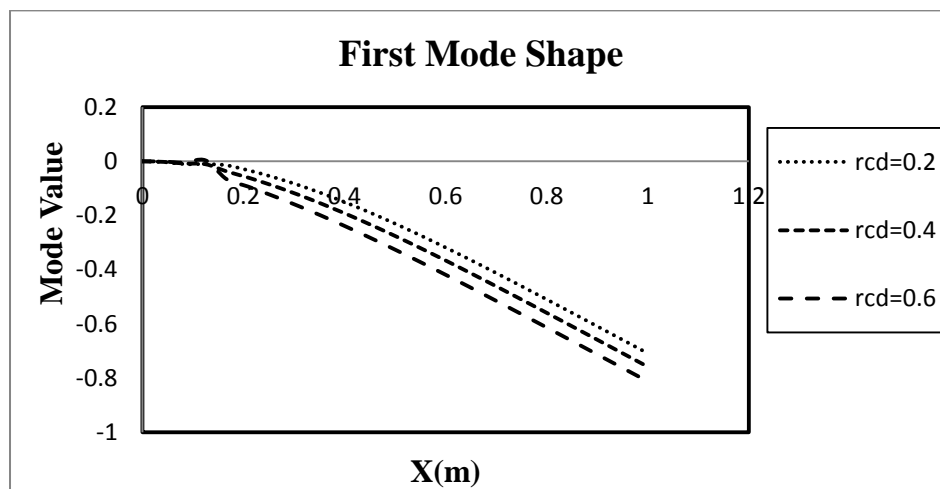


Figure 4.14 First mode shapes of cracked composite beam for $x=0.1L$ and relative cracked depth (rcd) = 0.2, 0.4, 0.6

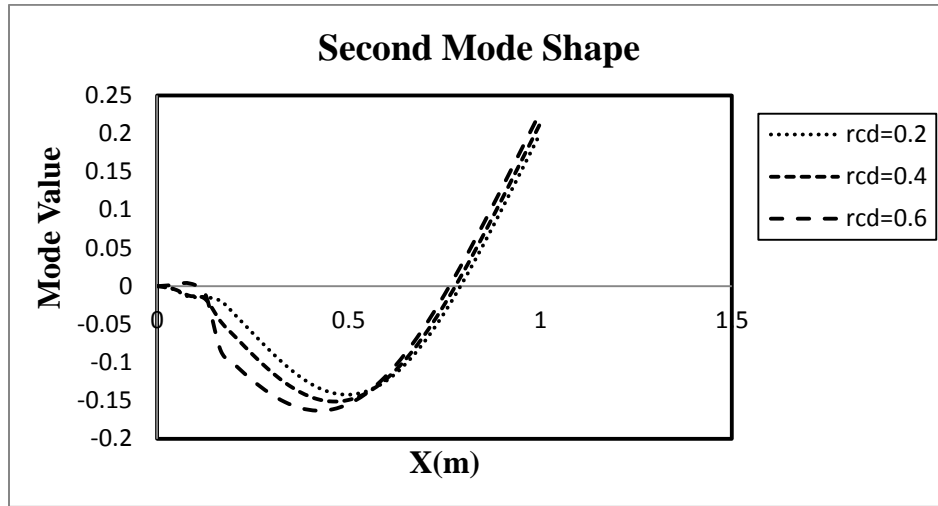


Figure 4.15 Second mode shapes of cracked composite beam for $x=0.1L$ and relative cracked depth (rcd) = 0.2, 0.4, 0.6

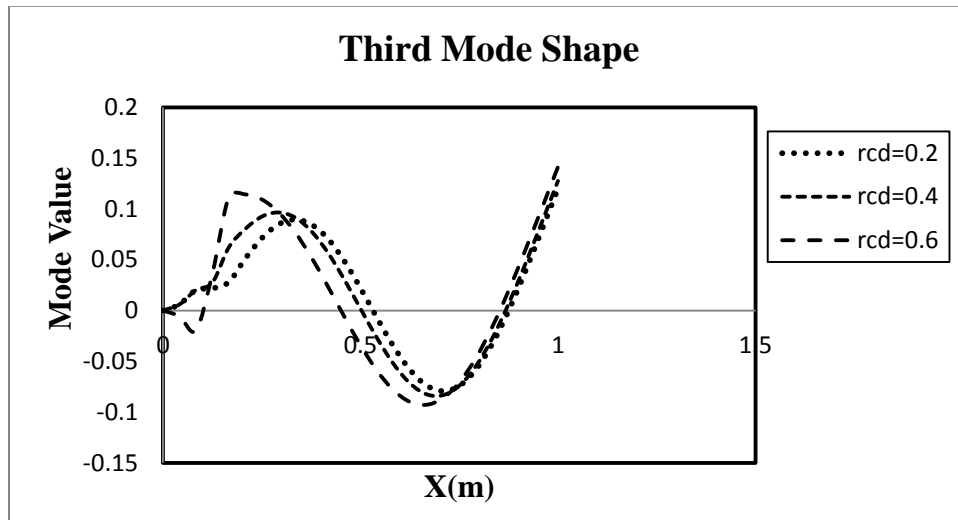


Figure 4.16 Third mode shapes of cracked composite beam for $x=0.1L$ and relative cracked depth (rcd) = 0.2, 0.4, 0.6

Thirdly, Figures 4.17 and 4.18 show the influence of the volume fraction of the fiber on the changes in the first two non-dimensional natural frequency of the analyzed cracked composite beam for the several values of the crack ratios (a/H). The calculations have been carried out for various values of the fiber volume fraction, depth of the crack (a/H) and the fiber angle ($\alpha=0^\circ$). The crack was located at a distance $x = 0.1L$ (m) from the fixed end of the beam. The decrease of the non-dimensional natural frequencies depends on the volume fraction of the fibers. The flexibility due to crack is high when the volume fraction of the fiber is between 0.2 and 0.8 and maximum when the fiber fractions is approximately 0.45. This is due to the fact that the flexibility of the composite beam due to crack is a function of the volume fraction of the fibers. Therefore, if the volume fraction of the fiber is between 0.2 and 0.8 and crack depth is getting higher, the frequency reductions are relatively high as seen in figure.

Table-4.12 Numerical result of First Non-dimensional natural frequencies of the cracked composite beam as a function of value fraction of fibers V for several values of the crack depth $a/H = 0.0, 0.2, 0.4$ and 0.6 (the angle of fibers $\alpha = 0$ degree, crack location $x/L = 0.1$)

Angle of fibers(degree)	Volume fraction of fiber	1 st Non-dimensional Frequency			
		Relative crack depth (a/h) = 0.0	Relative crack depth (a/h) = 0.2	Relative crack depth (a/h) = 0.4	Relative crack depth (a/h) = 0.6
0	0	2.4985	2.4829	2.2603	2.0032
	0.2	2.4985	2.2709	1.7452	1.3263
	0.4	2.4985	2.0618	1.4246	1.0028
	0.6	2.4985	2.0745	1.4332	1.0198
	0.8	2.4985	2.2683	1.7398	1.3265
	1.0	2.4985	2.4817	2.2580	2.0125

Table-4.13 Numerical result of Second Non-dimensional natural frequencies of the cracked composite beam as a function of value fraction of fibers V for several values of the crack depth $a/H = 0.0, 0.2, 0.4$ and 0.6 (angle of fibers $\alpha = 0$ degree, crack location $x/L = 0.1$)

Angle of fibers(degree)	Volume fraction of fiber	2 nd Non-dimensional Frequency			
		Relative crack depth (a/h) = 0.0	Relative crack depth (a/h) = 0.2	Relative crack depth (a/h) = 0.4	Relative crack depth (a/h) = 0.6
0	0	6.2303	6.0809	5.5362	5.2656
	0.2	6.2303	5.4703	4.9025	4.5044
	0.4	6.2303	5.1610	4.4687	4.1243
	0.6	6.2303	5.1704	4.4712	4.1031
	0.8	6.2303	5.3962	4.9132	4.5398
	1.0	6.2303	6.0825	5.5386	5.2208

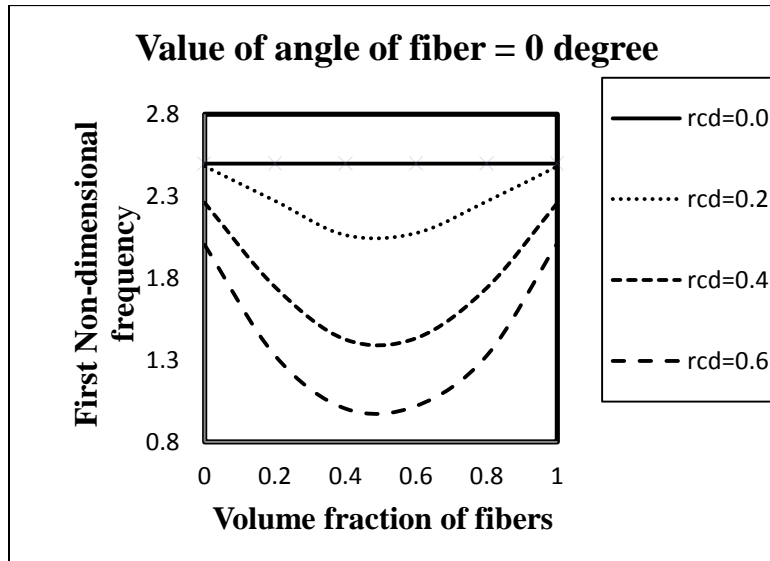


Figure 4.17 The First Non-dimensional natural frequencies of the cracked composite beam as a function of volume fraction of fiber V for several values of the crack depth $a/H = 0.0, 0.2, 0.4$ and 0.6 (the angle of fibers $\alpha = 0$ degree, crack location $x/L = 0.1$)

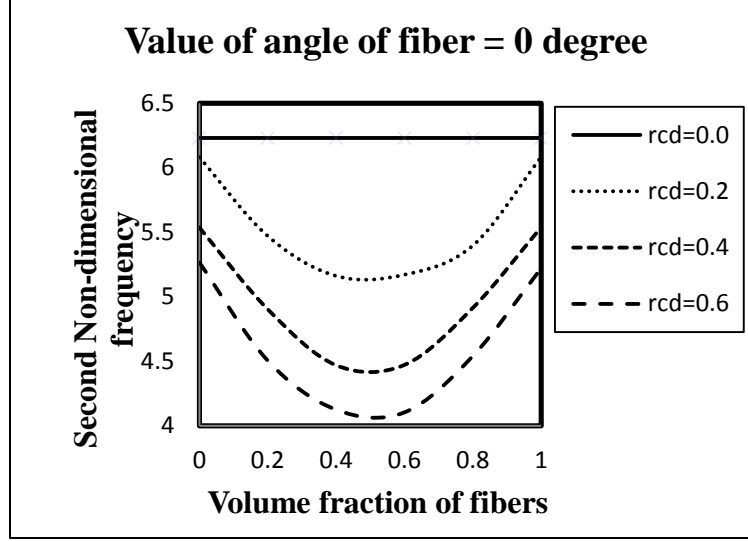


Figure 4.18 Changes in the Second Non-dimensional natural frequencies of the cracked composite beam as a function of volume fraction of fiber V for several values of the crack depth $a/H = 0.0, 0.2, 0.4$ and 0.6 (the angle of fibers $\alpha = 0$ degree, crack location $x/L = 0.1$)

Lastly, Figure 4.19, 4.20 show the plot of the ratio of the first two non-dimensional natural frequency of the cracked composite beam to the first two non-dimensional natural frequency of the non-cracked composite beam as a function of crack depth ratio (a/H) for crack position $x = 0.1L$ and volume fraction of fiber is equal to 0.1 . The relative changes are normalized according to the following relation

$$\omega_{relative} = \frac{\omega_{crack}}{\omega_{noncrack}} \quad (31)$$

where ω_{crack} denotes first non-dimensional natural frequency of the cracked composite beam, $\omega_{noncrack}$ denotes first non-dimensional natural frequency of the non-cracked composite beam

Table-4.14 First non-dimensional frequency ratios for different crack depth

Angle of fibers(degree)	Volume fraction of fiber	Frequency Ratio			
		RCD=0.0	RCD=0.2	RCD=0.4	RCD=0.5
0	0.1	1.582	0.855391	0.648475	0.587691
15		1.582	0.878415	0.673219	0.61044
30		1.582	0.948161	0.753332	0.684423
45		1.582	1.065357	0.903112	0.823612
60		1.582	1.230456	1.122819	1.028706
75		1.582	1.437624	1.367508	1.255673
90		1.582	1.575964	1.508766	1.385783

Table-4.15 Second non-dimensional frequency ratios for different crack depth

Angle of fibers(degree)	Volume fraction of fiber	Frequency Ratio			
		RCD=0.0	RCD=0.2	RCD=0.4	RCD=0.6
0	0.1	1.48341	0.949521	0.814194	0.640001
15		1.48341	0.970418	0.849881	0.655748
30		1.48341	0.982258	0.879118	0.672807
45		1.48341	1.05788	0.967248	0.750433
60		1.48341	1.149381	1.076545	0.855111
75		1.48341	1.28513	1.23085	0.982987
90		1.48341	1.47956	1.441413	1.138899

The natural frequencies of the cracked composite beam are lower than the non-cracked composite beam. These differences increase with the crack depth ratio. As shown in Figure 4.19, when the crack is perpendicular to the angle of fiber, the decrease in the first natural frequency is highest. As the angle of fiber increases, the relative changes in the first frequency reduce.

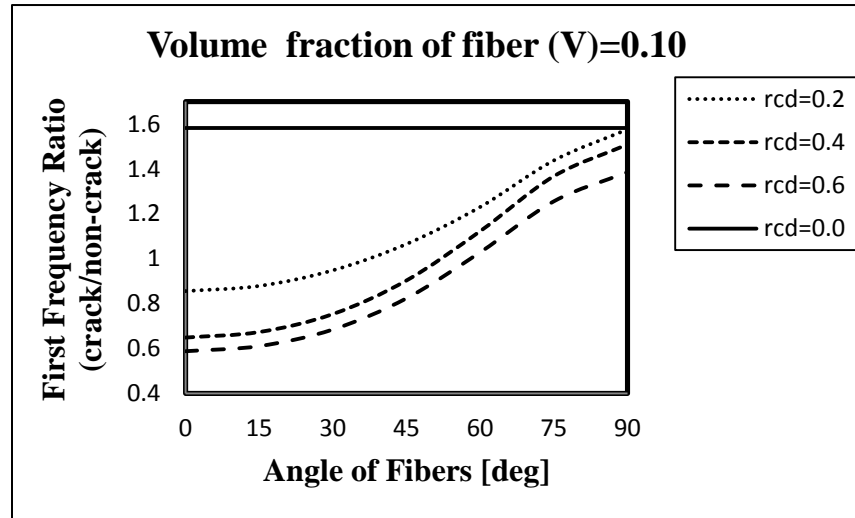


Figure 4.19 Relative changes in the first non-dimensional frequency ratios for different crack depth of the cracked composite beam

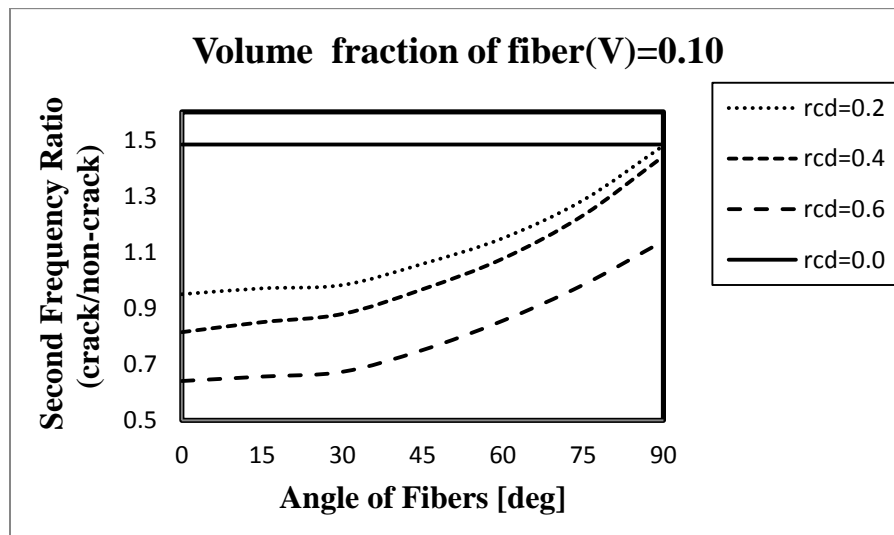


Figure 4.20 Relative changes in the second non-dimensional frequency ratios for different crack depth of the cracked composite beam

4.4.1(B) Vibration analysis of results of composite beam with multiple cracks

Quantitative results on the effects of various parameters on the vibration of composite cracked beams with multiple cracks are presented. The results are compared with previous studies and the present method is validated with published papers. The Finite element analysis is carried out for free vibration of a composite cracked beam for various crack positions and crack depth=0.2 for the example problem considered by Ozturk & Sabuncu (2005). In Figure 4.21 to 4.23, the variation of the first three lowest natural frequencies of the composite beam with multiple cracks is shown as a function of fiber orientation (α) for different crack locations l_i/L . In these figures, two cases, labeled as X and Y, are considered. In the model, the number of the cracks assumed to be three. The crack locations $l_1/L, l_2/L, l_3/L$ for the cases X and Y are chosen as (0.1, 0.2, 0.4), (0.6, 0.8, 0.9), respectively. For numerical calculations the volume fraction of fiber (V) and the crack depth (a/H) are assumed to be 0.10 and 0.2, respectively. The non-dimensional natural frequencies are normalized according to Eq. (29).

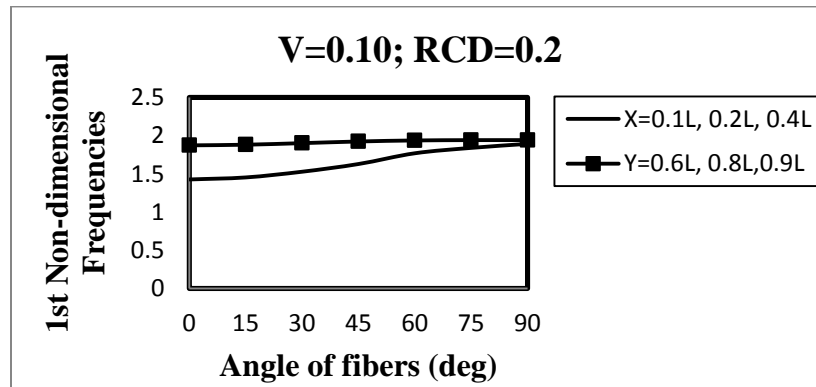


Figure 4.21 The first non-dimensional natural frequencies as a function of fiber orientation for the cases of three cracks located differently, as indicated a/H=0.2 and V=0.1

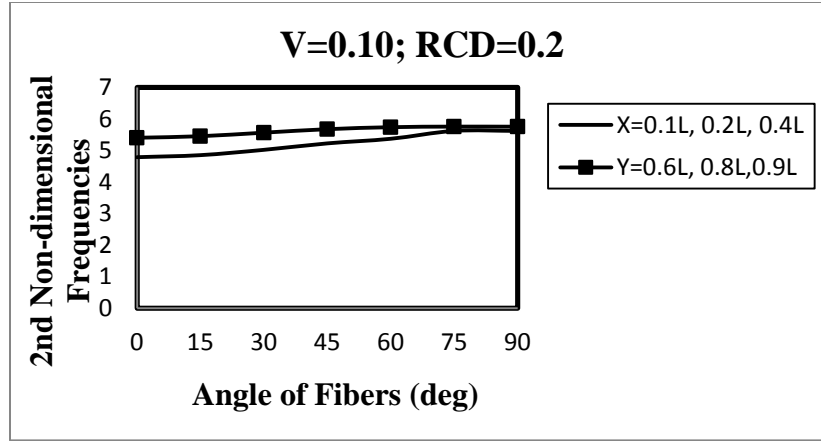


Figure 4.22 The second non-dimensional natural frequencies as a function of fiber orientation for the cases of three cracks located differently, as indicated $a/H=0.2$ and $V=0.1$

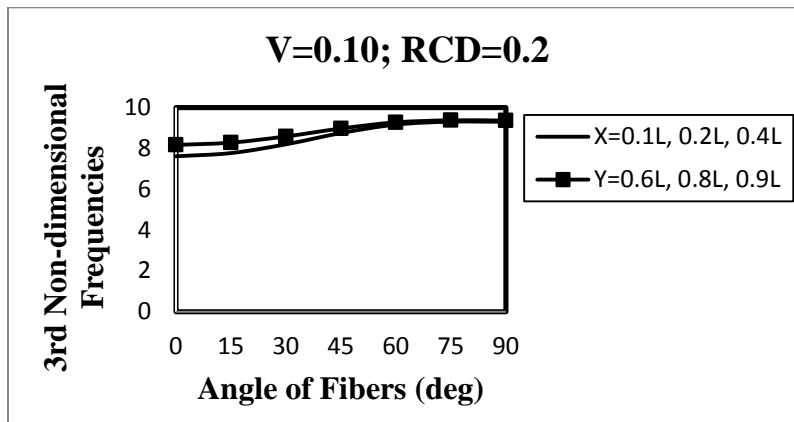


Figure 4.23 The third non-dimensional natural frequencies as a function of fiber orientation for the cases of three cracks located differently, as indicated $a/H=0.2$ and $V=0.1$

It can be clearly seen from the Figure 4.21 to 4.23 that, when the cracks are placed near the fixed end the decreases in the first natural frequencies are highest, whereas when the cracks are located near the free end, the first natural frequencies are almost unaffected. It is concluded that the first, second and third natural frequencies are most affected when the cracks located at the near of the fixed end, the middle of the beam and the free end, respectively.

Similarly the study is extended for buckling analysis of a cantilever composite beam with a crack for the same beam taken by Ozturk & Sabuncu (2005).

4.4.2 Buckling analysis of results of composite beam with single crack

The buckling analysis is done for the same beam as considered by Ozturk & Sabuncu (2005) and Reddy (1997) for different crack locations and crack depths. The results are tabulated in table 4.16 and plotted in the Figure 4.24 to 4.27. The calculations have been carried out for 10% volume fraction of the fiber and the angle of fibers varying from 0 to 90 degrees. From the table 4.16, it is clear that the non-dimensional buckling load of the beam reduces from 4.9984 to 4.7154 with introduction of a crack at 0.1L and relative crack depth of 0.2. The non-dimensional buckling load decreases substantially from 4.7154 to 3.1330 with increase of relative crack depth from 0.2 to 0.6 due to decrease in stiffness. Similarly the non-dimensional buckling load decreases with increase of relative crack depth from 0.2 to 0.6 for other cases of the crack position i.e. 0.1L, 0.2L, 0.4L, 0.6L and 0.8L. The variation of non-dimensional buckling loads of cantilever composite beam with crack location for different relative crack depth (0.2 to 0.6), when angle of fiber = 0 degree is shown in Figure 4.25. It is observed that the non-dimensional buckling load increases from 4.7154 to 4.9640 with increase of x/L from 0.1 to 0.8 for relative crack depth = 0.2. For relative crack depth 0.6 the non-dimensional buckling load increases from 3.1330 to 4.3844 when the location of crack shifts from 0.1L to 0.8L. It means the non-dimensional buckling load of a cracked cantilever composite beam is higher if the crack is near the free end than near the fixed end and non-dimensional buckling load decreases with increase in relative crack depth. For a given crack depth it increases as crack location moves from fixed end to free end. Buckling load decreases with increase in angle of fibers and is maximum at 0

degree. This is due to the fact that for 0 degree orientation the buckling plane normal to the fibers is of maximum stiffness and for other orientations stiffness is less hence buckling load is less.

Table-4.16 Buckling loads for different crack locations for a composite cracked beam for angle of fiber = 0, 30, 60 and 90 degrees

Relative Cracked depth (a/H)	Angle of fibers (degree)	Crack position				
		x = 0.1L	x = 0.2L	x = 0.4L	x = 0.6L	x = 0.8L
0.2	0	4.7154	4.7649	4.8753	4.9241	4.9640
0.4		4.0126	4.1812	4.4494	4.6547	4.8769
0.6		3.1330	3.2406	3.5529	3.9873	4.3844
0.2	30	1.1461	1.2740	1.4347	1.5828	1.6142
0.4		0.4037	0.5562	0.7016	1.0428	1.3763
0.6		0.2961	0.4376	0.6292	0.8714	1.1906
0.2	60	0.3507	0.3591	0.3733	0.3816	0.3871
0.4		0.2159	0.2479	0.2743	0.3193	0.3539
0.6		0.1687	0.2100	0.2343	0.2741	0.3243
0.2	90	0.1892	0.1909	0.1957	0.1976	0.1994
0.4		0.1369	0.1452	0.1565	0.1718	0.1849
0.6		0.1101	0.1178	0.1321	0.1484	0.1709

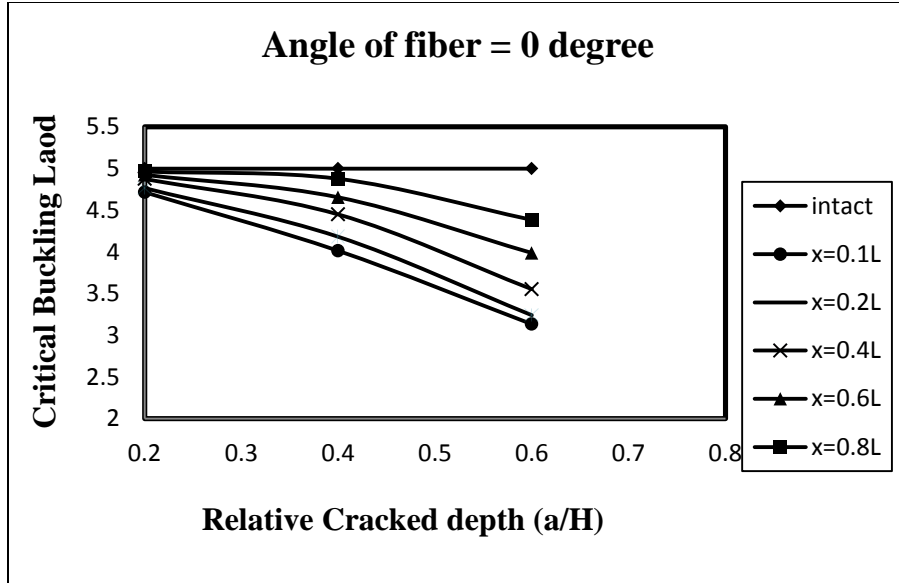


Figure 4.24 Critical buckling load vs. relative crack depth for different crack location
when angle of fiber = 0 degree

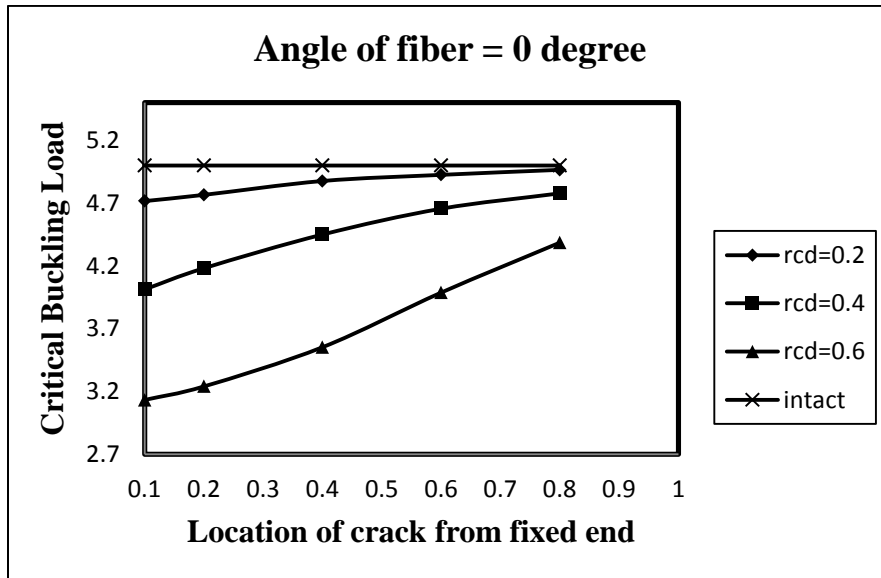


Figure 4.25 Critical buckling load vs. crack location for different relative crack depth when
angle of fiber = 0 degree

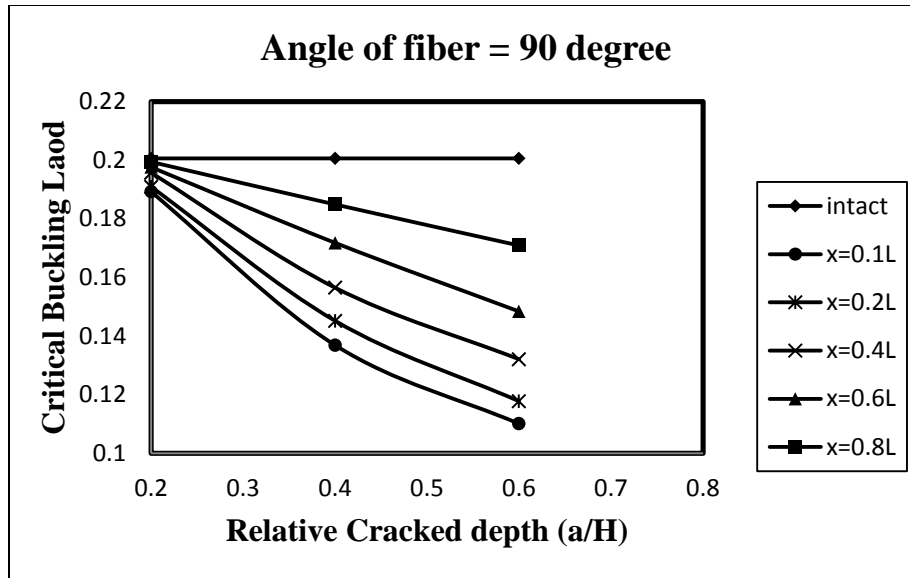


Figure 4.26 Critical buckling load vs. relative crack depth for different crack location
when angle of fiber = 90 degree

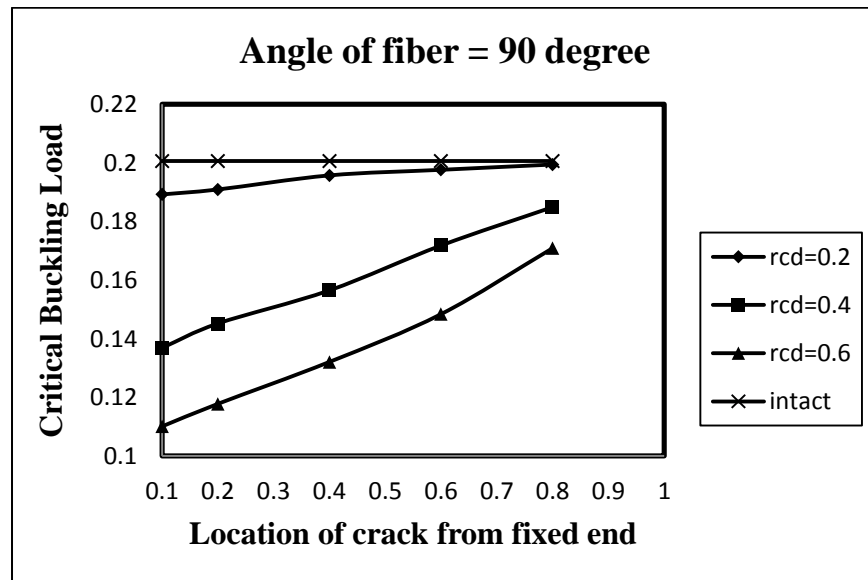


Figure 4.27 Critical buckling load vs. crack location for different relative crack depth
when angle of fiber = 90 degree

5.1 Conclusion

The following conclusions can be made from the present investigations of the composite beam finite element having transverse non-propagating one-edge open crack. This element is versatile and can be used for static and dynamic analysis of a composite or isotropic beam.

- 1) From the present investigations it can be concluded that the natural frequencies of vibration of a cracked composite beam is not only the functions of the crack locations and crack depths but also the functions of the angle of fibers and the volume fraction of the fibers. The presence of a transverse crack reduces the natural frequencies of the composite beam.
- 2) The rate of decrease in the natural frequency of the cracked composite beam increases as the crack position approaches the fixed end.
- 3) The intensity of the reduction in the frequency increases with the increase in the crack depth ratio. This reduction in natural frequency along with the mode shapes of vibrations can be used to detect the crack location and its depth.
- 4) When, the angle of fibers (α) increase the values of the natural frequencies also increase. The most difference in frequency occurs when the angle of fiber (α) is 0 degree. This is due to the fact that the flexibility of the composite beam due to crack is a function of the angle between the crack and the reinforcing fibers.
- 5) The effect of cracks is more pronounced near the fixed end than at far free end. It is concluded that the first, second and third natural frequencies are most affected when the

cracks located at the near of the fixed end, the middle of the beam and the free end, respectively.

- 6) The decrease of the non-dimensional natural frequencies depends on the volume fraction of the fibers. The non-dimensional natural frequency is maximum when the volume fraction of fiber is approximately 45%. This is due to the fact that the flexibility of a composite beam due to crack is a function of the volume fraction of the fibers.
- 7) Buckling load of a cracked composite beam decrease with increase of crack depth for crack at any particular location due to reduction of stiffness.
- 8) When, angle of fibers increase the values of the buckling loads decrease. This is due to the fact that for 0 degree orientation of fibers, the buckling plane normal to the fibers is of maximum stiffness and for other orientations stiffness is less hence buckling load is less.

5.2 Scope of future work

1. The vibration and stability results obtained using this formulation can be verified by conducting experiments.
2. The dynamic stability of the composite beam with cracks
3. Static and dynamic stability of reinforced concrete beam with cracks.
4. The dynamic stability of beam by introducing slant cracks (inclined cracks) in place of transverse crack.

REFERENCES

REFERENCES

- 1) Adams R. D., Cawley, P. C., Pye J. and Stone J. (1978). A vibration testing for non-destructively assessing the integrity of the structures. *Journal of Mechanical Engineering Sciences* 20, 93-100.
- 2) Banerjee J. R. (2001). Frequency equation and mode shape formulae for composite Timoshenko beams. *Composite Structures* 51 (2001) 381-388.
- 3) Binici B. (2005) Vibration of beams with multiple open cracks subjected to axial force. *J Sound Vib*; 287(1-2):277–95.
- 4) Broek D. *Elementary Engineering Fracture Mechanics*. Martinus Nijhoff; 1986.
- 5) Chandrupatla T. R., Belegundu A. D. Introduction to finite elements in engineering. New Jersey: Prentice-Hall; 1991.
- 6) Dimarogonas A.D. (1996), *Vibration of Cracked Structures: A State of the Art Review*. Engineering Fracture Mechanics, 55(5), 831-857.
- 7) Ghoneam S. M. (1995). Dynamic analysis of open cracked laminated composite beams. *Composite Structures* 32 (1995) 3-11.
- 8) Gounaris G.D., Papadopoulos CA, Dimarogonas AD. (1996). Crack identification in beams by coupled response measurement. *Comput Struct*; 58(2):299–305.
- 9) Goyal Vijay K., Kapania Rakesh K. (2008). Dynamic stability of laminated beams subjected to non-conservative loading. *Thin-Walled Structures* 46 (2008) 1359– 1369.
- 10) Hamada A. Abd El-Hamid (1998). An investigation into the eigen-nature of cracked composite beams. *Composite Structure* Vol. 38, No. 1 - 4, pp. 45-55.
- 11) Jones R. M. Mechanics of composite materials. Taylor & Francis Press; 1999.
- 12) Kaihong Wang, Daniel J. Inmana & Charles R. Farrar (2005). Modeling and analysis of a cracked composite cantilever beam vibrating in coupled bending and torsion. *Journal of Sound and Vibration* 284 (2005) 23–49.

- 13) Kisa Murat (2003). Free vibration analysis of a cantilever composite beam with multiple cracks. *Composites Science and Technology* 64 (2004) 1391–1402.
- 14) Krawczuk M, (1994). A new finite element for the static and dynamic analysis of cracked composite beams. *Composite & Structures* Vol. 52. No. 3, pp. 551-561, 1994.
- 15) Ostachowicz W.M. and Krawczuk M (1991). Analysis of the effect of cracks on the natural frequencies of a cantilever beam. *Journal of Sound and Vibration* (1991) 150(2), 191-201.
- 16) Krawczuk M., Ostachowicz W. and Zak A. (1997). Modal analysis of cracked, unidirectional composite beam. PIh \$0022-1694(97)00045-0S1359-8368(96)00081-9.
- 17) Krawczuk M., and Ostachowicz W.M., (1995). Modelling and Vibration Analysis Of a Cantilever Composite Beam with a Transverse Open Crack. *Journal of Sound and Vibration* (1995) 183(1), 69-89.
- 18) Lu Z.R., Law S.S. (2009). Dynamic condition assessment of a cracked beam with the composite element model. *Mechanical Systems and Signal Processing* 23 (2009) 415–431.
- 19) Manivasagam S. & Chandrasekharan K. (1992). Characterization of damage progression in layered composites. *Journal of Sound and Vibration* 152, 177-179.
- 20) Nikpour K. and Dimarogonas A.D. (1988). Local compliance of composite cracked bodies. *Journal of Composite Science and Technology* 32,209-223.
- 21) Nikpour K. (1990). Buckling of cracked composite columns. *Journal of Solids and Structures* 26, 371-1386.
- 22) Oral S. (1991). A shear flexible finite element for non-uniform laminated composite beams. *Computers and Structures* 38, 353-360.
- 23) Ozturk Hasan, Sabuncu Mustafa (2005). Stability analysis of a cantilever composite beam on elastic supports. *Composites Science and Technology* 65 (2005) 1982–1995.
- 24) Przemieniecki J. S. *Theory of Matrix Structural Analysis*. London: McGraw Hill first edition (1967).
- 25) Przemieniecki J. S. and Purdy D. M. (1968). Large deflection and stability analysis of two dimensional truss and frame structure. AFFDL-TR-68-38.
- 26) Reddy J N. *Mechanics of laminated composite plates theory and analysis*. New York: CRS Press; 1997.

- 27) Sih G. C. and Chen E. P. (1981) in Mechanics of Fracture. *Cracks in composite materials* London: Martinus Nijho first edition.
- 28) Timoshenko S. (1940), *Theory of Plates and Shells*, McGraw Hill Book Company Inc., New York & London.
- 29) Vinson J. R. and Sierakowski R. L. *Behaviour of Structures Composed of Composite Materials*. Dordrecht: Martinus Nijho first edition (1991).
- 30) Wauer J. (1991). Dynamics of cracked rotors: a literature survey. *Applied Mechanics Reviews* 17, 1-7.
- 31) Wang Kaihong and Inman Daniel J. (2002). Coupling of Bending and Torsion of a Cracked Composite Beam. Center for Intelligent Material Systems and Structures Virginia Polytechnic Institute and State University Blacksburg, VA 24061-0261.
- 32) Yang J., Chen Y. (2008). Free vibration and buckling analyses of functionally graded beams with edge cracks. *Composite Structures* 83 (2008) 48–60.
- 33) Zak A., Krawczuk M. and Ostachowicz W. M. (2000). Numerical and experimental investigation of free vibration of multilayered delaminated composite beams and plates. *Composite Mechanics* 26 (2000) 309-315.
- 34) Zhou L., Huang Y. (2006). Crack effect on the elastic buckling behavior of axially and eccentrically loaded columns. *Structure Eng. Mech.* 2006; 22(2):169–84.

APPENDIX - A

$$\begin{matrix} S_{11} & m^4 & 2m^2n^2 & 2m^2n^2 & n^4 & S_{11} \\ S_{13} & = m^3n & 2(mn^3 - m^3n) & -2(m^3n + mn^3) & -mn^3 & \times S_{12} \\ S_{33} & m^3n & -2m^3n & (m^4 + n^4 - 2m^3n) & m^3n & S_{33} \\ & & & & & S_{22} \end{matrix}$$

Thus,

$$S_{11} = S_{11}m^4 + 2 S_{12} + 2S_{33} m^2n^2 + S_{22}n^4$$

$$S_{13} = (S_{11} - S_{12} - 2S_{33})m^3n + S_{12} - S_{22} - 2S_{33} mn^3$$

$$S_{33} = (S_{11} - 2S_{12} + S_{22} - 2S_{33})m^3n + S_{33} m^4 + n^4$$

The terms S_{ij} corresponding with the materials principal axes x_1, y_1 are determined by the following formulae:

$$S_{11} = \frac{E_{11}}{(1 - \nu_{12}^2 E_{22} E_{11})}$$

$$S_{22} = S_{11} E_{22} E_{11}$$

$$S_{12} = \nu_{12} S_{22}$$

$$S_{33} = G_{12}$$

whereas the gross mechanical properties of the composite, $E_{11}, E_{22}, G_{12}, \nu_{12}$ and ρ are calculated by using the following formulae (the subscript f denotes fibre, the subscript m denotes matrix and E, G, ν and ρ are the modulus of elasticity, the modulus of rigidity, the Poisson ratio and the mass density respectively).

$$\rho = \rho_f V + \rho_m (1 - V)$$

$$E_{11} = E_f V + E_m (1 - V)$$

$$E_{22} = E_m \left[\frac{E_f + E_m + \frac{E_f - E_m}{E_f - E_m} V}{E_f + E_m - \frac{E_f - E_m}{E_f - E_m} V} \right]$$

$$\nu_{12} = \nu_f V + \nu_m (1 - V)$$

$$\nu_{23} = \nu_f V + \nu_m (1 - V) \left[\frac{1 + \nu_m - \frac{\nu_{12} E_m}{E_{11}}}{1 + \nu_m^2 - \frac{\nu_m \nu_{12} E_m}{E_{11}}} \right]$$

$$G_{12} = G_m \left[\frac{G_f + G_m + \frac{G_f - G_m}{G_f - G_m} V}{G_f + G_m - \frac{G_f - G_m}{G_f - G_m} V} \right]$$

$$G_{23} = \frac{E_{22}}{2(1 + \nu_{23})}$$